THESIS FOR THE DEGREE OF LICENTIATE OF ENGINEERING

**Development of a Method for Accelerated Ageing of Cementitious Materials Used in Repositories for Nuclear Waste**

AREZOU BABAAHMADI

Department of Civil and Environmental Engineering
CHALMERS UNIVERSITY OF TECHNOLOGY
Gothenburg, Sweden 2013

Development of a Method for Accelerated Ageing of Cementitious Materials Used in Repositories for Nuclear Waste

AREZOU BABAAHMADI

Department of Civil and Environmental Engineering

Cover:
The Calcium Leaching Process: Decalcification of Cementitious Materials

TO MY BROTHER

Development of a Method for Accelerated Ageing of Cementitious Materials Used in Repositories for Nuclear Waste

Thesis for the Degree of Licentiate of Engineering

AREZOU BABAAHMADI
Department of Civil and Environmental Engineering
Chalmers University of Technology

ABSTRACT

The Swedish nuclear fuel and waste management company (SKB), is required to validate the service life prediction of the concrete structures in nuclear waste repositories. Considering the repository being in contact with water , the decalcification process of cementitious materials although being very slow can during the very long operational lifetime of the repository (up to 100000 years), cause the degradation of chemical and mechanical properties of the concrete structures. In order to predict the long-term service life of the structures without extrapolating short-term experimental results, methods that accelerate the leaching process of calcium from cementitious materials are required. In this work the development process of an electro-chemical migration method for acceleration of the calcium leaching from cementitious specimens is presented. The method enables ageing of cementitious specimens with sufficiently large sizes suitable for testing mechanical and transport properties. In this method, the cementitious specimen is placed in an electrochemical cell as a porous path way through which ions can migrate at a rate far higher than diffusion process. The results show that, by a careful adjustment of the experimental parameters such as the magnitude of electrical field and choice of anolyte and catholyte solutions, an effective leaching of calcium with an acceleration factor of >600 can be obtained. According to instrumental analysis the chemical and mineralogical properties of the treated specimens are comparable with the characteristics of the aged specimens in natural decalcification process.


Key Words: Acceleration, Calcium Leaching, Cementitious Materials, Transport Properties, Diffusion, Long-Term Performance

# CONTENTS

# PREFACE

The project entitled "Ageing of Cementitious Materials for Storage of Nuclear Waste" is founded by Swedish Nuclear Fuel and Waste Management Company (SKB) and started from August 2010. The presented work is the results of two and a half years of research in this project. This work was carried out at the division of Building Technology, Department of Civil and Environmental Engineering, Chalmers University of Technology.

I would like to thank my supervisors Professor Tang Luping and Associate Professor Zareen Abbas, whom I am very grateful for providing me with their experiences and answering endless flow of my questions.

My sincere gratitude goes to Professor Gunnar Gustafson who introduced me this project. May he rest in peace and his memory will stay with us.

I also wish to thank Dr. Per Mårtensson at SKB and Dr. Peter Cronstrand for their constructive comments and suggestions during this work.

My co-workers and colleagues at Division of Building Technology are greatly appreciated for their friendship and all the support.

And last but not least, I would like to thank my parents for all their love and support during these years of being far from home.


AREZOU BABAAHMADI
February 1, 2013

# ABBREVIATIONS AND NOTATIONS

| | |
|---|---|
| C | CaO |
| $C_2S$ | Dicalcium Silicate |
| $C_3A$ | Tricalcium Aluminate |
| $C_3S$ | Tricalcium Silicate |
| $C_4AF$ | Tetracalcium Aluminoferrite |
| CH | Portlandite |
| Clab | The interim storage facility for nuclear fuel |
| C-S-H | Calcium silicate hydrates |
| EDAX | Energy dispersive X-Ray spectroscopy |
| H | $H_2O$ |
| HCP | hydrated cement paste |
| IC | Ion Chromatography |
| S | $SiO_2$ |
| SEM | Scanning Electron Microscopy |
| SFL | The final repository for long-lived radioactive waste |
| SFR | The final repository for short- lived radioactive waste |
| SKB | The Swedish nuclear fuel and waste management company |
| SSM | The Swedish Radiation Safety Authority |
| Sv | Sievert (stochastic biological effects of ionizing radiation) |
| XRD | X-Ray Diffraction |
| XRF | X-Ray Fluorescence spectroscopy |
| | |
| $c$ | concentartion |
| $D$ | Diffusion coefficient |
| $F$ | Faraday number (C/mol) |

| | |
|---|---|
| $i$ | van 't Hoff factor |
| $I$ | Current (A) |
| $M$ | Molarity |
| $M$ | Molar weight of substance (g/mol) |
| $m$ | Mass of substance (g) |
| $n$ | number of dissociated ions |
| $R$ | Gas constant (J K-1 mol-1) |
| $S$ | Surface area in contact with leachate |
| $T$ | Absolute Temperature |
| $t$ | time (seconds) |
| $u$ | ion mobility |
| $V$ | Sample volume |
| $z$ | Valance number of the charged substance |
| $\alpha$ | degree of dissolution |
| $v_m$ | velocity of the charged substance |
| $\varphi$ | Porosity |

# MAIN PUBLICATIONS

PAPER I.   A. Babaahmadi, L. Tang and Z. Abbas, Development of an Accelerated Ageing Method for Cementitious Materials in Long-Term Contact with Water, SUBMITTED TO CEMENT AND CONCRETE RESEARCH JOURNAL

PAPER II.   A. Babaahmadi, L. Tang , Z. Abbas and J. Boman, Mineralogical Properties of Cementitious Materials Undergoing Accelerated Decalcification, SUBMITTED TO CEMENT AND CONCRETE COMPOSITES JOURNAL

## OTHER RELEVANT PUBLICATIONS BY AUTHOR

i.   A. Babaahmadi, L. Tang and Z. Abbas, Electrochemical migration technique to accelerate ageing of cementitious materials. proceedings of the Workshops on long-term performance of cementitious barriers and reinforced concrete in nuclear power plant and radioactive waste storage and disposal, NUCPERF 2012, Cadarache, France

ii.   A. Babaahmadi, L. Tang and Z. Abbas, Ageing process of cementitious materials: Ion transport and diffusion coefficient. Concrete Repair, Rehabilitation and Retrofitting III - Proceedings of the 3rd International Conference on Concrete Repair, Rehabilitation and Retrofitting, ICCRRR 2012, Cape Town, South Africa, pp. 369-374. ISBN/ISSN: 978-041589952-9

iii.   A. Babaahmadi, L. Tang and Z. Abbas, A study of the accelerated ageing process of cementitious materials. Advances in Construction Materials through Science and Engineering, Hong Kong, RILEM PRO 79 pp. 93.

iv.   A. Babaahmadi, L. Tang, Z. Abbas and G. Gustafson, Ageing of cementitious materials for storage of nuclear waste. Hameelinna, Finland, Nordic Concrete Research, Publication No. 43 pp. 429-432.

v.    P. Cronstrand, A. Babaahmadi, L. Tang and Z. Abbas, Electrochemical leaching of cementitious materials: an experimental and theoretical study, Proceedings of the 1st International Symposium on Cement-Based Materials for Nuclear Wastes, NUMCEM 2011, Session 3 (Paper O344) pp. 15.

# 1    Introduction

## 1.1 Nuclear waste management in Sweden

Nuclear power has been an alternative energy production solution for Swedish power industry since about 40 years ago. In Sweden all produced radioactive waste and spent nuclear fuel in nuclear facilities are required to manage and dispose in such a way to maintain the maximum required safety for the human and environment.

The Swedish nuclear fuel and waste management company (SKB) was initiated in 1970s as a partnership between nuclear power companies in Sweden. The assignment is to manage the disposal of radioactive waste according to the obligations from the time that the waste leaves the nuclear power plants. The obligations regarding the final disposal of radioactive waste are regulated based on certain permits and guidelines issued by the government as well as "Nuclear Activities Act "(1984:3), "The Radiation Protection Act" (1988:220) and "The Act on Financial Measures for the management of the residual products from nuclear activities" (2006:647). It should be noted that the Swedish radiation safety authority (SSM) has control on SKB's activities [1].

The geological disposal of the nuclear fuel and radioactive waste is the most applicable and the safest solution for the waste management. In order to design the final repository for the geological disposal of nuclear waste, SKB has considered several parameters [1]:

- The repository should be located in long term stable environment and situated in bedrock having no future economic interest.
- Multiple engineered barriers should be designed for different radioactivity levels in waste and the barriers should be from natural occurring materials with long term stability.
- There should be no need of future monitoring or maintenance after the closure of the repository.

The current disposal facilities in Sweden include:

- The interim storage facility for nuclear fuel (Clab) situated near Oskarshamn
- The final repository for short lived radioactive waste (SFR) located in Forsmark.

3

Currently there are also plans for extension of SFR and also to build a new repository for long lived radioactive waste (SFL) and a repository for spent nuclear fuel.

The disposal of radioactive waste is based on the radioactivity level and life time of the waste. There exist very low, low, intermediate and high level classes of radioactivity for the waste. Very low level waste is short lived waste and it will be deposited in surface repositories. The low and intermediate level waste is divided into short lived and long lived waste. The long lived part will eventually be stored in SFL and the short lived part is deposited in SFR. The spent nuclear fuel which is considered as long lived waste will be deposited in spent fuel repository.

In order to assure the safety of the final disposal of radioactive waste in SFR and also in order to demonstrate the measures taken in to account within the design of the future planned disposal facilities, risk assessment analysis should be undertaken. A safety assessment should undergo several steps, but the most important section is identification of the probable future courses of events for long term evaluation of the repository. It should be noted that safety assessments for long term disposal facilities are demonstrated based on SSM's regulations (Swedish Radiation Safety Authority):

- Protection of human health shall be ensured by fulfillment of a risk criterion stipulating that "the annual risk of harmful effects after closure does not exceed $10^{-6}$ for a representative individual in the group exposed to the greatest risk". The "harmful effects" means cancer and hereditary defects. According to SSM, this risk limit is equivalent to a dose limit of about $1.4 \cdot 10^{-5}$ Sv/year, which is about 1% of the natural background radiation in Sweden.
- As far as environmental protection is concerned, biological effects of ionizing radiation due to releases of radioactive material from a repository to important habitats and ecosystems shall be described based on available knowledge.
- The consequences of intrusion into a repository shall be reported and the protective capability of the repository after intrusion shall be described.
- SSM requires a more detailed assessment for the first 1000 years after closure of the final repository than for subsequent periods.
- The safety assessments shall comprise features, events and processes which can lead to the dispersion of radioactive substances after closure.

- A safety assessment shall comprise as long a time span as barrier functions are required, but at least ten thousand years.
- Reporting of the following is required:
  - Methods for system description and system development;
  - Methods for selection of scenarios, including a main scenario that takes into account the most probable changes in the repository and its environment,
  - The applicability of models, parameter values and other premises used in the analyses, and
  - Management of uncertainties and sensitivity analyses.
- With respect to the analysis of post-closure conditions, it requires a description of the evolution in the biosphere, the geosphere and the repository for the selected scenarios.

## 1.2     Engineered barriers in repositories of nuclear waste

As it has been pointed out the design of the final repository requires engineered barriers according to the level of radioactivity of the waste. The current repository for the radioactive waste, SFR, in Sweden, consists of several parts with respect to the radioactivity level of the waste. The Silo (intermediate waste), BMA (intermediate waste), 1BTF and 2BTF (dewatered ion exchange resins) and BLA (low level waste) are the included parts. The facility is a hard rock system located 60 meters beneath the sea. The silo as of containing the most reactive part of the waste is designed with multi-layers of engineered barriers. The waste container is considered as the first barrier which will be embedded in concrete. The reinforced concrete walls provide additional barriers. Furthermore between the concrete walls and the rock as the outer barrier layer, a bentonite layer is engineered providing higher safety. The BMA vault is structured using rock as the loadbearing parts and in situ casted reinforced concrete is used as the slab and flooring and the walls and the whole structure is constructed on a base of shot rock leveled with gravel. The 1BTF and 2BTF are concrete tank repositories and the BLA vault has a concrete floor and rock walls.

Considering the construction of the repository concrete was extensively used in the repository not only as an engineered barrier, but also to fulfill required structural

strength. Cementitious materials having high pH buffering capacity, implying good mechanical properties and low diffusivity are considered as a suitable alternative construction material in repositories of nuclear waste. The used concrete in SFR has around 300-350 kg/m$^3$ cement content, 0.7 aggregate volume fraction and a Water-Cement ratio of about 0.5-0.6 [2, 3].

The safety assessment of the cementitious concrete barriers as one of the primary measures to prevent release of radionuclides to the environment is of great importance. The service life predictions of the cementitious materials have been a major topic since application of these materials in the repositories. In order to account for the effect of climate changes on the service life of the facilities the predictions should be made for a service life more than 100000 years [1]. The performance assessments require detailed multidisciplinary analysis regarding the long term chemical and mechanical properties of cementitious materials. The method to perform the safety assessments undergoes several steps: identifications of all the events and factors of importance, description of the safety functions to overcome probable risks, selection of the scenarios with the higher probability of failure and finally risk evaluation. As of dealing with a complicated and coupled processes influencing the performance of the barriers the current knowledge and experimental data are not sufficient to demonstrate the effectiveness of the engineered barriers [4] and more assessment is necessary in order to improve the understanding of the long-term performance of the barriers.

## 1.3    Initiation of the project and the goals

In order to broaden the knowledge and understanding of the long-term degradation of the cementitious materials as well as to provide data bases accounting for the changes in the chemical and mechanical properties of the cementitious materials after degradation, the project called "Ageing of cementitious materials for storage of nuclear waste" was initiated and funded by SKB. The project is defined as a PhD work performed at Chalmers University of Technology, Department of Civil and Environmental Engineering, Division of Building Technology. The primary objectives is to investigate the mechanical and chemical properties of the aged cementitious materials undergoing calcium leaching as the major deterioration factor

regarding the cementitious concrete barriers in nuclear waste repositories. The specific goals included in the project descriptions are:

- Laboratory investigation of various accelerated aging tests in order to find suitable regimes for manufacturing the aged cementitious materials without significantly distorting the properties of the material from the natural aging processes.

- Laboratory investigation of physical and chemical properties of "young" and aged cementitious materials, including mechanical properties, transport properties (diffusivity), binding (adsorption) capacities, surface complexation (charge) behaviors, and chemical and mineralogical stabilities. The predictions should have a perspective of 100000 years as the service life.

- Thermodynamic modeling of aging of cementitious materials used in the exposure environment (main contribution from Vattenfall Power consultant)

- Synthesis and analysis of the test and modeling results with the intention of establishing a mechanism-based (chemo-mechanical coupled) model for longevity prediction of concrete for storage of nuclear waste.

# 2 Durability of Cementitious Materials

## 2.1 Cement and cement hydration

Cement is an essential part of the concrete. It hardens after mixing with water through several chemical reactions and functions as a binder. More than 95% of the cement which is used around the world is Portland cement [4]. The main constituents of Portland cement are calcium oxide (CaO) and silicon dioxide ($SiO_2$), both of which exist in earth's crust as calcium carbonate and sand. The Portland cement powder has a grain size between 2 and 80 μm, it is grey in color and has a relative density of about 3.14 $g/cm^3$. The chemical compositions of cement consist of Tricalcium Silicate ($C_3S$), Dicalcium Silicate ($C_2S$), Tricalcium Aluminate ($C_3A$) and Tetracalcium Aluminoferrite ($C_4AF$), which are known as the four phases of cement. In order to calculate the compound composition of cement Bogue equation [5] is used. After mixing cement with water the hydration starts. The rate of hardening is very considerable after about 2-4 hours and a very rapid strength is gained after a few days. However after this time the hardening continues with a decreasing rate for at least a few months. It should be noted that the hydration reactions never end and in order to show the level of reactions, hydration degree is used as an indicator. The hydration of two phases of cement, $C_3S$ and $C_2S$, are of great importance as of contributing to the most of engineering properties of hydrated cement paste (HCP) like strength and stiffness. The hydration reactions are presented in Equations (2.1) and (2.2) below:

$$2C_3S + 6H \longrightarrow C_3S_23H + 3CH \tag{2.1}$$

$$2C_2S + 4H \longrightarrow C_3S_23H + CH \tag{2.2}$$

where,

C: CaO

S: $SiO_2$

H: $H_2O$

CH: $Ca(OH)_2$

As it is presented in Equation (2.1) and (2.2), the main portion of hydrated products are C-S-H ($C_3S_2H_3$) and CH known as Portlandite. The C-S-H part of the HCP

11

contributes to the strength properties and the CH part together with other hydroxides produced during the hydration (NaOH and KOH) provides alkaline characteristics (pH: 12.5-13) having a great influence on durability of cementitious materials. Figure 2-1, illustrates the main constituents of HCP after few weeks of hydration.
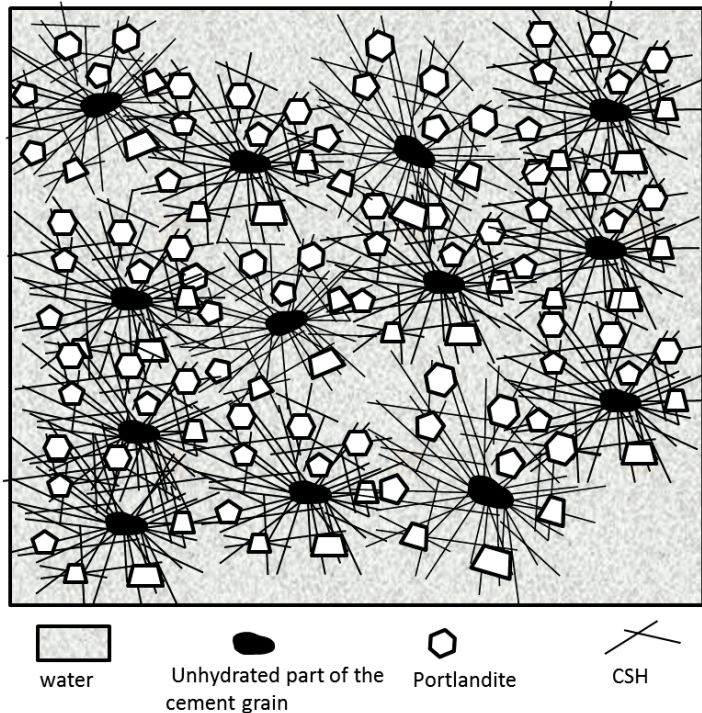


*Figure 2-1. The main constituents of HCP after a few weeks of hydration*

## 2.2    Degradation of cementitious materials

The exchange of ions between the environment and the hydrated cement paste cause alterations to the microstructural properties of cementitious materials.

One of a very well-known scenarios concerning service life of specifically reinforced concrete structures is the chloride ingress. Exposure of cementitious materials to chloride ions will cause reaction with aluminate phases in the paste and formation of Friedel's salt ($3Cao.Al_2O_3.CaCl_2.10H_2O$) [6-9], which creates possibility of expansion and cracking. The major influence of the presence of chlorides is destruction of the protective passive layer on the steel surface causing initiation of corrosion. The corrosion products contribute stress around the rebar and consequently damage the concrete cover. However, the chloride concentration of the groundwater around repositories is too low to form Friedel's salt (<0.1 M [10]).

Another well-known case causing destructions in cementitious systems is carbonation. The gaseous carbon dioxide penetrates in to HCP matrix causing production of $HCO_3^-$ and $CO_3^{2-}$ which will react with dissolved calcium and the reaction leads to precipitation of $CaCO_3$ (Calcite). Although the production of calcite causes reduction of the material porosity and increases the retention of the constituents [11], the consumption of the Portlandite causes a pH drop in the system. The pH drop can affect the protective passive layer of the reinforced steel.

Sulfate attack is another degradation problem. The reaction of the sulfate ions with the cement system leads to production of:

- Gypsum ($CaSO_4.2H_2O$)
- Ettringite ($[Ca_3Al(OH)_6 \cdot 12H_2O]_2 \cdot (SO_4)_3 \cdot 2H_2O$)
- Thaumasite ($Ca_3[Si(OH)_6 \cdot 12H_2O] \cdot (CO_3) \cdot SO_4$)

These products can cause expansion, spalling and severe degradation [12-14].

Another factor causing the major deterioration in long-term service life of the cementitious barriers in nuclear waste repository [15, 16] is related to long term contact of cementitious systems with water. The low calcium content of the water in the surrounding environment causes a concentration gradient which leads to dissolution and eventually leaching of the calcium from the hydrated cement matrix. As it has been mentioned earlier that C-S-H and CH parts of the HCP system contribute to the strength and durability properties and therefore decalcification affects the chemical and mechanical properties of the cementitious materials.

## 2.3 Decalcification of cementitious materials

As explained in previous section the major process causing degradation of cementitious materials in long-term contact with water is decalcification of the hydrated cement system. It is shown in several studies that the calcium leaching process is governed by a coupled dissolution/diffusion process [17]. The kinetics of an ionic diffusion process can be presented in a simplified way, Equation (2.3) [18].

$$\phi(x,t)\frac{\partial c(x,t)}{\partial t} = D(x,t)\frac{\partial^2 c(x,t)}{\partial x^2} - \frac{\partial c_s(x,t)}{\partial t} \qquad (2.3)$$

where,

$c(x,t)$: Ca$^{2+}$ concentration in the liquid phase

$c_s(x,t)$: Content of Ca$^{2+}$ in the solid phase

$\phi(x,t)$: Porosity

$D(x,t)$: Diffusion coefficient

Equation (2.3) indicates that a major factor in a diffusive transport process is the concentration gradients. Due to a low concentration of calcium ions in the water, dissolution of calcium hydroxides followed by diffusive transport of calcium ions, leaching of calcium, occurs. The loss of calcium leads to dissolution of Portlandite followed by decalcification of C-S-H. Figure 2-2, illustrates the decalcification process of HCP. Based on the study by Adonet [19] the degraded material has a layered system which consist of different zones separated by precipitation/dissolution fronts and continuous decalcification of C-S-H. It is shown that decalcification changes the pore structure of hardened cement paste[20] due to dissolution of Portlandite increasing the porosity. Moreover, it is shown that the increase in the pore water has influence on mechanical properties of cementitious materials [21, 22].
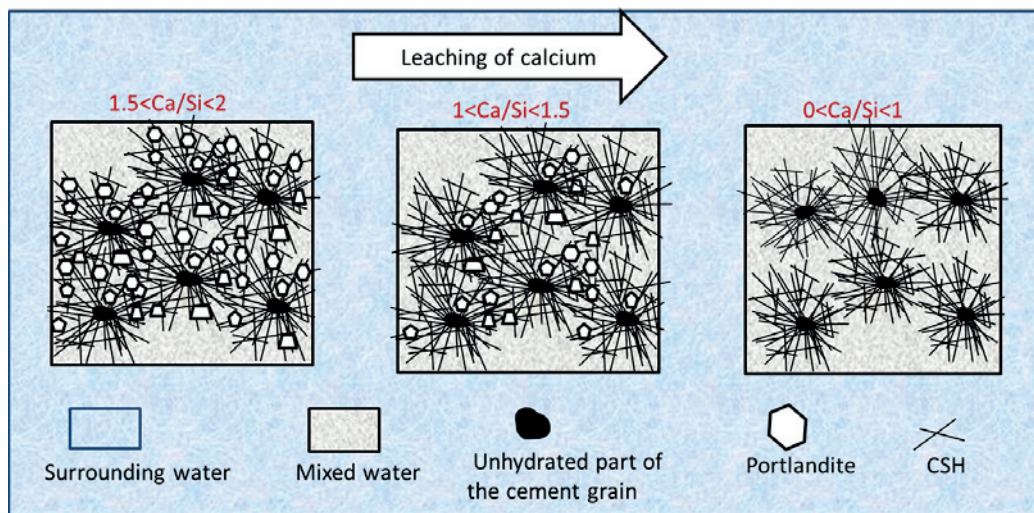


*Figure 2-2. Decalcification of hydrated cement paste*

## 2.4    Accelerated ageing and available experimental test methods

In order to model the leaching process several test methods have been developed, mainly based on immersion of the cement-based specimens in water [14, 18]. However as of dealing with a process with a very slow kinetics, long experimental times are required. In order to facilitate the studies concerning decalcification and also to prevent extrapolating short-term experimental data for prediction of long-term degradation effects, several acceleration methods have been proposed, which are classified in literature in two categories, electrical and chemical accelerations.

A well-known acceleration method is electrical migration. There exist a few studies in the literature based on the migration concept [23-25]. According to definition of migration it is possible to move charged substances with the application of electrical field. The charged substances move under the gradient of the electrical field toward a certain direction according to their valance state. The average velocity of the movement is defined according to Equation (2.4) below:

$$\upsilon_m = u \cdot \frac{\partial \psi}{\partial x} \tag{2.4}$$

where,

$\upsilon_m$: Velocity of the charged substance

u: ion mobility

According to the Einstein relation ion mobility can be defined as Equation (2.5) in following:

$$u = D \cdot \frac{z \cdot F}{R \cdot T} \tag{2.5}$$

where,

$D$: diffusion coefficient

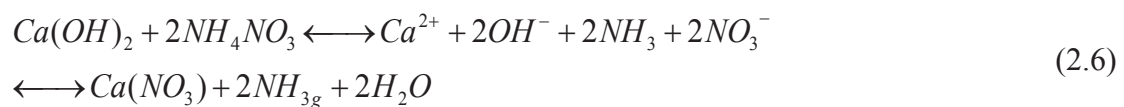$z$: Valance number of the charged substance

15

$F$: Faraday number $F$= 96485 C/mol

$R$: Gas constant

$T$: Temperature

In a study performed by Saito et al. (1992) which is considered as a reference electrical acceleration method in the literature, a disc of mortar sample with a diameter of 50 mm and thickness of 10mm is placed between two glass vessels containing water as electrolyte. A constant potential of 25 V is applied during the experimental time and carbon electrodes are used as cathode and anode. The experimental results are promising considering the overall decrease of Ca/Si ratio during the experimental time. However the size of the aged samples is not suitable for further mechanicals tests. Moreover, the changes of the pH level in electrolyte solutions in the course of experiment were not reported, which indicates possible scenarios of acidic characteristics of the anolyte solution due to production of $H^+$ ions around anode.

Another category of accelerated leaching is application of aggressive solutions. A very strong chemical acceleration method presented in the literature is immersion of samples in concentrated ammonium nitrate solution [20, 21, 26]. As it is reported by Heukamp et al. (2000), the application of ammonium nitrate solution favors dissolution of calcium hydrates due to formation of highly soluble $Ca(NO_3)_2$ along with the consumption of the $OH^-$ ions in calcium hydroxides (Equation (2.6)).

$$Ca(OH)_2 + 2NH_4NO_3 \longleftrightarrow Ca^{2+} + 2OH^- + 2NH_3 + 2NO_3^-$$
$$\longleftrightarrow Ca(NO_3) + 2NH_{3g} + 2H_2O$$

(2.6)

In this method cylindrical paste specimens with the size of Ø11.5×60 mm are immersed in an oscillating box containing 6M ammonium nitrate solution. It is indicated that in order to reach a quasi-steady state, 45 days of experimental time is required and during this time the propagation of the dissolution front is $2mm/\sqrt{day}$. Although the acceleration rate is very high, the size of the aged samples limits further physical tests like diffusivity or permeability.

16

Another chemical method accelerating the decalcification process was developed based on the effect of the pH of solution in contact with the cementitious materials [27]. However applying solutions of very low pH to reach high acceleration rates may destruct the whole hydrates system, which distorts the real leaching process.

# 3 Development of an acceleration method

It has been discussed in previous chapters that, in order to improve the understanding of long-term deterioration of cementitious systems undergoing calcium leaching, development of an effective acceleration method with sufficiently large sample sizes has been the major goal in this project. This chapter presents the development process in this study. The initial set-up design of the method was regulated according to literature recommendations. However initial design was gradually refined in order to achieve the most efficient combination of adjustable settings enabling leaching of calcium without introducing unexpected damage in the specimen due to temperature increase, osmotic pressure or chemical attack. The chronicle adjustment of several set-up parameters was made based on the results and observed problems from a series of experimental trials.

## 3.1    Test specimens

In order to facilitate the chemical and mineralogical analysis, cement paste was used in the development process of the method. Swedish Portland cement for civil engineering (CEM I 42.5N BV/SR/LA) was used as cementitious binder. The chemical composition of the cement is listed in Table 3-1. The cement was mixed with distilled water at a water-cement ratio of 0.5. Fresh cement paste was cast in acrylic cylinders with an internal diameter of 50 mm and length of 250 mm. The ends of the cylinders were sealed with silicone rubber stops. In order to produce homogenized specimens, the cylinders containing fresh paste were rotated longitudinally at a rate of 12-14 rpm for the first 18-24 hours of hydration. Afterwards the rubber stops were removed and the cylinder ends sealed with plastic tape. The specimens were then stored in a moist plastic box for more than 6 month before cut to cylinders with the size of Ø50×75 mm for use as specimens in the migration test.  In order to prevent specimens from significant carbonation, the bottom of the plastic box was filled with saturated lime water. To avoid possible carbonation effect, the end portion of about 10-20 mm was cut off prior to the specimen cutting.

*Table 3-1. Chemical characteristics of Swedish CEM I 42.5N BV/SR/LA*

| Chemical formulation | CaO | SiO₂ | Al₂O₃ | Fe₂O₃ | MgO | Na₂O | K₂O | SO₃ | Cl |
|---|---|---|---|---|---|---|---|---|---|
| Percentage | 64 | 22.2 | 3.6 | 4.4 | 0.94 | 0.07 | 0.72 | 2.2 | 0.01 |

## 3.2 Initial design of the electrochemical migration method

### 3.2.1 Electrochemical migration theory

Under a gradient of external electrical potential, the cations such as $Na^+$, $K^+$, $Ca^{2+}$ in the pore solution will move towards the cathode whilst the anions such as $OH^-$ will move towards the anode. The actual movement of ionic species can be described by the Nernst-Plank equation:

$$J_i = -D_i \frac{\partial c_i}{\partial x} - c_i D_i \frac{z_i F}{RT} \cdot \frac{\partial \Psi}{\partial x} \tag{3.1}$$

where $J$ is the flux of ions, $D$ denotes the diffusion coefficient, $c$ is the molar concentration, $R$ is the gas constant, $T$ is the absolute temperature, $x$ is the distance, $z$ is the valence of ions, $F$ is the Faraday constant, and $\Psi$ is the electrical potential including both the so called counter electrical potential due to different mobilities between anions and cations and the imposed external electrical potential across the anode and the cathode. The subscript $i$ represents specific type of ions. In the right side of equation (3.1) the first term describes diffusion, whilst the second term describes migration process. Equation (3.1) has been used by Tang [28] in the development of the rapid chloride migration test which was adopted as the Nordic standard NT BUILD 492 [29].

Under a certain gradient of external electrical potential, the migration current is the sum of ions moving in the pore solution, that is,

$$I = AF\sum_j z_j J_j = AF\sum_j z_j \left( -D_j \frac{\partial c_j}{\partial x} - c_j D_j \frac{z_j F}{RT} \cdot \frac{\partial \Psi}{\partial x} \right) \tag{3.2}$$

where $I$ is the migration current and $A$ is the cross-sectional area of specimen. The subscript $j$ denotes various types of ions. Combining equations (3.2) and (3.1) one can obtain the following equation:

$$J_i = -D_i \frac{\partial c_i}{\partial x} + \frac{D_i z_i c_i \left( \sum_j D_j z_j \frac{\partial c_j}{\partial x} + \frac{I}{AF} \right)}{\sum_j D_j z_j^2 c_j} \tag{3.3}$$

More detailed description of the electrochemical migration theory has been presented by Cronstrand et al. [30].

From the above equations it can be seen that, either under a constant potential as shown in equation (3.2) or under a constant current as shown in equation (3.3), the specific ion transport will be influenced by the coexisting ions, depending on individual ionic mobility or diffusivity and concentration gradient. Therefore, to develop an electrochemical migration method for calcium leaching, we have to try to reduce the flax contributions from the coexisting ions while to increase the concentration gradient of calcium ions.

### 3.2.2 Experimental set-up design

As illustrated in Figure 3-1, the initial set-up design of the electrochemical migration method is an inspiration based on the rapid chloride migration method developed by Tang (1996) [28]. As illustrated in Figure 3-1, a paste specimen with a size of Ø50×75 mm was sealed around its curved surface and placed between two electrolyte solutions (electrical cells) as a porous medium enabling movement of ions which are enforced by the electrical gradient. The sealant was made of silicon rubber tube which was 2-3 times longer in height than the specimen's, providing an empty volume of about 300 ml used as the anolyte container. A plastic box with capacity of 30 liters was used as the catholyte container. The cathode was made of stainless steel and was mounted on a plastic support in a similar way as described in NT BUILD 492 [29]. The anode was produced using a titanium mesh. The cells were connected to an

external potential supplier with adjustable current and potential. In order to avoid a temperature-induced mechanical destruction of the specimen the potential or the current applied to the specimen was controlled to prevent significant elevation in temperature due to the Joule effect. The voltage and current changes were registered using a data-log system during the experiment. Considering deionized water which was used as electrolyte solutions in many previously reported electrical acceleration methods [22-24, 31], the initial experimental trial was designed utilizing deionized water as catholyte. On the other hand, considering the fact that anolyte solution should supply the system with positive charged substances compensating for the migration of the positive ions from the cementitious specimen, in order to facilitate leaching of calcium ions, 1 M $LiNO_3$ solution was used as anolyte. The selection of this salt as the first alternative was legitimized according to the fact that lithium ions were neither present in the initial pore solution nor reactive with the cement hydrates, and also application of a nitrate salt had the advantage of facilitating dissolution of calcium hydroxides due to production of highly soluble $Ca(NO_3)_2$, although the likelihood of penetration of nitrates into the specimen was very low because of the electrical gradients.
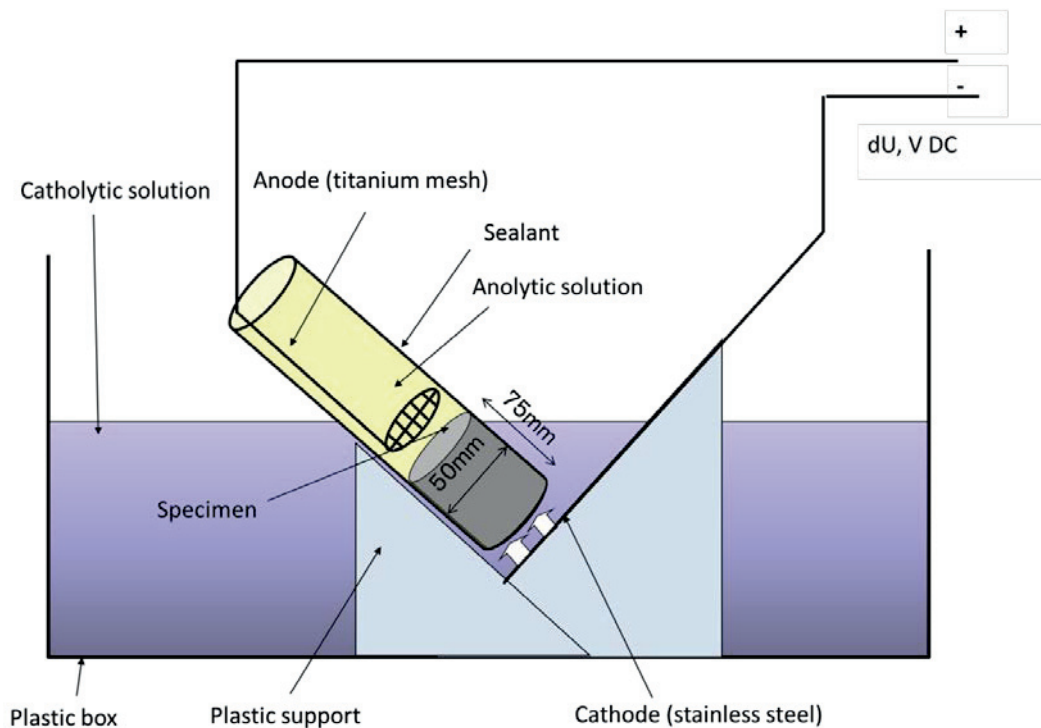


*Figure 3-1. Preliminary Set-up design of electrochemical migration method*

Despite of the above mentioned consideration, implementation of the outlined design set-up in the course of the first experimental trial indicated that after 150 hours of experimental time the resistance level inside the specimen increased promptly, as will be seen in Figure 3-2. A plausible explanation for this behavior is that, when the initial alkaline ions $K^+$ and $Na^+$ in the pore solution near the cathodic side of the specimen were leached out, no sufficient $Li^+$ ions from the anodic side had been reached the cathodic side for compensation of the leached alkaline ions, while the $Ca^{2+}$ ions balanced with $OH^-$ ions at a much lower concentration (about 0.046 N) than the initial alkaline concentration (about 0.5 N) and formed a high resistant zone inside the specimen, which made it practically impossible to further accelerate the leaching process.

## 3.3    Improvement of conductivity

As mentioned in the previous section, it was realized after the initial experimental trial that insufficient amount of lithium ions close to the cathodic side would be the reason to the generation of high resistances. Therefore, the implemented amount of anolyte solution should be in accordance with the expected amount of leaching. Considering Portlandite, being leached out first in the course of decalcification [19] and also considering the calcium content inside the specimen as presented in Table 3-2, (0.7 moles of Portlandite for 128 g of cement paste), the implemented amount of lithium ions should be around 1.4 moles.

In order to investigate if the low concentration of anolyte solution is the actual reason to the increase of resistance level, the second trial with implementation of 3 M $LiNO_3$ was carried out. However the chronicle change of the resistance was not showing any improvement.

*Table* **3-2.** *Initial calcium and silica contents in a cement paste specimen (Considering C₃S₂H₃ as the composition of C-S-H)*

| Total | Componenet | mole/gr cement | mole/specimen (229 g cement/specimen) |
|---|---|---|---|
| Calcium content | C-S-H | 0.00145×3=0.00435 | 0.332×3=0.996 |
| | CH | 0.00303 | 0.693 |
| | Total | 0.00738 | 1.689 |
| Silica content | C-S-H | 0.00145×2=0.0029 | 0.332×2=0.664 |

Nevertheless, even though the insufficiency of lithium ions in the cathodic side is a plausible cause of high resistances another fact is that there should be an agent favoring dissolution of Portlandite. When using only water there is no negative ion carrying the current rather than hydroxides, which will be balanced with limited amount of $Ca^{2+}$ ions from Portlandite and as a result after a short time when much more conductive potassium and sodium ions are leached out from the specimen the leaching process will stop. Therefore, in order to facilitate dissolution of calcium and also to reduce the amount of hydroxide ions produced around the cathode, a low concentration of lithium nitrate solution (0.3 M) was used as catholyte in the third experiment. It should be noted that in this trial the anolyte was not refreshed and certain amount of solid $LiNO_3$ salt was added to the solution to recharge the properties. The function of lithium nitrate solution as an agent favoring dissolution of calcium hydroxides [20] has been discussed in chapter 2. However, an important factor is to facilitate migration of nitrate ions in to the specimen which can happen if the $OH^-$ ions produced at the cathode can be neutralized. So the pH level of the solution should be monitored and well-kept below 9. The pH level was monitored in the course of Trial 3 and in case of a change in pH level solid $NH_4NO_3$ was added to the catholyte solution to provide more nitrate ions. However, in case of a rise in the pH value the unconsumed $OH^-$ ions could be consumed with H+ ions produced from ammonium according to Equation (3.4).

$$NH_4^+ \longleftrightarrow NH_{3aq} + H^+ \qquad pk_a NH_4^+ = 9.25 \qquad\qquad (3.4)$$

The selection of a low concentrated ammonium nitrate solution was in consideration of preventing aggressive effects of high concentrated ammonium nitrate solution, causing un-prioritized leaching of calcium silica hydrates. Figure 3-2, illustrates chronicle changes of resistances inside the specimen in the course of above mentioned three trials, it can be seen that implication of ammonium nitrate solution as catholyte in Trial 3 led to gradual decrease of the resistance level inside the specimen. Table 3-3 presents the set-up parameters applied in the course of first three trials.

*Table 3-3. Set up parameters applied in the course of first three trials*

| Trial number | Anolyte | Catholyte | Current/potential |
|---|---|---|---|
| 1 | 1 M LiNO$_3$ without refreshment | Initially demineralized water | 0.5 A constant current |
| 2 | 3 M LiNO$_3$ with certain refreshment | Initially demineralized water + Ca(OH)$_2$ (in order to reduce CO$_3^{2-}$ in the solution) | 0.2 A constant current |
| 3 | 3 M LiNO$_3$ with certain number of addition of solid LiNO$_3$ powder | 0.3 M NH$_4$NO$_3$ with an addition of solid NH$_4$NO$_3$ | 0.2 A constant current |
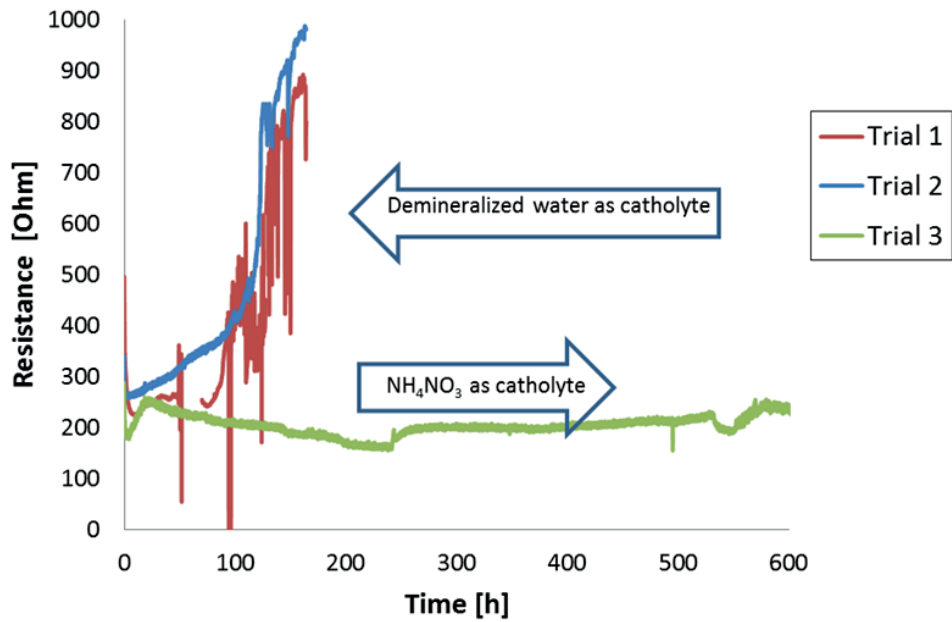
**Figure 3-2. Ohmic resistance across the specimens in Trials 1 to 3**

## 3.4 Refinement of initial design to reach efficient leaching rate of calcium

As of dealing with an accelerated leaching method, the rate of acceleration is of great importance. Moreover in order to reach the highest acceleration factor all the parameters should be regulated based on the most efficient set-up design. In order to study the effect of anolyte solution on the rate of acceleration the effect of ammonium nitrate and lithium hydroxide solution was also analyzed through a course of trials. It should be noted that according to the observations from Trial 3, implying an anolyte solution with a concentration of 3 M, led to considerable increase in the volume of the anolye solution, which disturbed the experiment. The selection process of anolyte concentration is described in the following.

### 3.4.1 Concentration of anolyte solution: osmotic pressure

A plausible explanation to justify the volume change of anolyte solution is the high ionic gradient between catholyte and anolyte solutions which leads to high osmotic pressures and considerable flow of solution towards anolyte. The osmotic pressure is defined according to Equation (3.5), presented below:

$$\Pi = i \cdot M \cdot R \cdot T \tag{3.5}$$

where,

$M$: Molarity

$R$: Gas constant = 8.314 (J K$^{-1}$ mol$^{-1}$)

$T$: Absolut temperature

$i$: van 't Hoff factor which is defined according to Equation (3.6):

$$i = 1 + \alpha(n-1) \tag{3.6}$$

where,

$\alpha$: degree of dissolution

$n$: number of dissociated ions

According to this equation and also considering the flow of liquids in a porous medium, a volume increase about 60ml is expected during 24 hours.

In order to control the osmotic pressure and also to supply enough amounts of lithium ions to the specimen the initial set-up design was improved using 2M salt solution as anolyte.

### 3.4.2   Type of anolyte solution

In order to study the function of different types of salt as anolyte and the effect of this variability on leaching rate of calcium ions, several experiments were formulated using 2 M LiNO$_3$, LiOH, NH$_4$NO$_3$, NaOH and KOH solutions as anolyte. It should be noted that since sodium and potassium are present inside the specimen the experiments with application of sodium and potassium hydroxides started with a lithium salt solution for the first 150 hours (enough experimental time for leaching of original Na and K ions from the specimen) of the experiment which followed by addition of these hydroxides to the initial anolyte solution in the form of solid powder salt, in order to recharge the properties of the anolyte solution. Moreover, ammonium nitrate solution was also used as anolyte in order to study the efficiency of this salt in

favoring the dissolution of calcium hydroxides. Table 3-4 summarizes the differences in set-up design of a sequence of experimental trials performed in this study.

*Table 3-4. Experimental parameters*

| Trial number | Anolyte | Catholyte | Current/potential |
|---|---|---|---|
| 4 | I. 2 M $NH_4NO_3$ with an addition of solid<br>II. 2 M $LiNO_3$ with an addition of solid | 0.3 M $NH_4NO_3$ | 50 V constant potential |
| 5 | I. 2 M LiOH, the solution is renewed at certain intervals<br>II. 2 M $LiNO_3$ with an addition solid<br>III. 2 M $LiNO_3$, the solution is renewed at certain intervals | 0.3 M $NH_4NO_3$ with an addition of solid $NH_4NO_3$ if the pH value is raised. | 50 V constant potential |
| 6 | 2 M $LiNO_3$ with refreshment of solution | 0.3 M $NH_4NO_3$ with an addition of solid $NH_4NO_3$ if the pH value is raised. | 50 V constant potential |
| 7 | 2 M LiOH with refreshment of solution | 0.3 M $NH_4NO_3$ with an addition of solid $NH_4NO_3$ if the pH value is raised. | 50 V constant potential |
| 8 | 2 M $LiNO_3$ with addition of KOH in powder form | 0.3 M $NH_4NO_3$ with an addition of solid | 50 V constant potential |
| 9 | 2 M LiOH with addition of NaOH in powder form | 0.3 M $NH_4NO_3$ with an addition of $HNO_3$ | 0.25 A constant current |

Figure 3-3, illustrates the leaching rate of calcium ions in the course of Trial 4-9 versus applied electrical field. Comparing the leaching rate in different trials it can be concluded that application of sodium and potassium hydroxide salts decreases the rate.
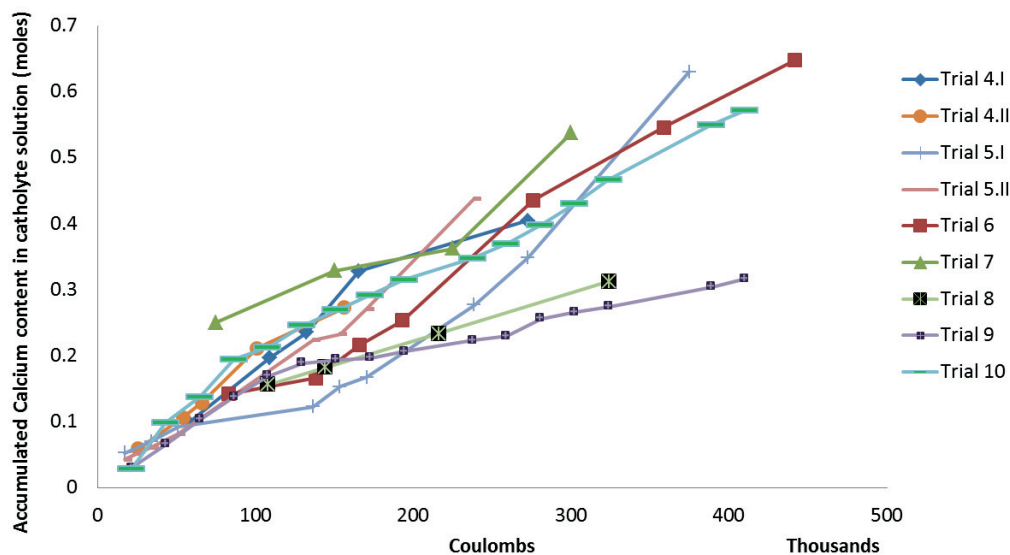


*Figure 3-3. Accumulated calcium contents in the catholyte solution (moles) in time*

This indicates that the sodium or potassium ions carried more current than the lithium ions in the migration process. The competitive migration between lithium, sodium and potassium is mainly explained by the differences in their ionic size and surrounding water layer. $Li^+$ ion has crystallographic radius 0.07 nm whereas $Na^+$ and $K^+$ ions have crystallographic radii 0.102 and 0.134 nm, respectively. This means that Li ion has high surface charge density and, therefore, it is strongly hydrolyzed in water and acquires large size. Recently effective radius of Li, Na and K were determined in their chloride and nitrate salts by comparing the mean activity coefficients calculated by Monte Carlo (MC) simulations with the experimental data [32]. The effective radius of Li was found to be 0.21 nm compared with Na and K which had effective radii of 0.168 and 0.134 nm respectively. This also indicates that $K^+$ ions do not have hydrated water molecules around it whereas sodium has some, but it is less than the amount of water molecules around $Li^+$ ions. $Li^+$ ions having comparatively small radius and thus strong surface charge concentration have thick water layer surrounding them, when available in solution form, which will consequently cause

31

low tendency to diffuse or migrate. The thicker water layer around Li in salt solution will consequently cause low tendency to diffuse or migrate.

Moreover, as illustrated in Figure 3-4 (Trial 9), the experimental results with application of NaOH, indicated possible generation of alkali-silica reaction close to the anodic side.

Although the results show similar trends of leaching rate through application of $LiNO_3$, LiOH and $NH_4NO_3$, the visual characteristics of the specimens undergoing acceleration show extensive destructions in the specimen close to the anodic side, which indicates aggressive effects of the anolyte solutions, Figure 3-4.



*Figure 3-4. Visual characteristics of the treated specimens*

This is explained by the fact that $H^+$ generated at the anode has an aggressive effect on the specimen and if applying an anolyte solution with alkaline characteristics, this can be prevented. However the anolyte solution should be recharged frequently with respect to the produced amount of $H^+$ ions at the anode. Since this regulation was not applied to the previous mentioned experimental trials, even the trials with application of LiOH as anolyte were still showing destructions of the specimen close to the

anode. The reaction of alkaline anolyte with the $H^+$ ions could be approved in the experiments as a whitish foam layer produced on top of the anolyte solution, which shows agitation of anolyte solution and production of bubbles due to acid base reaction was observed, Figure 3-5.
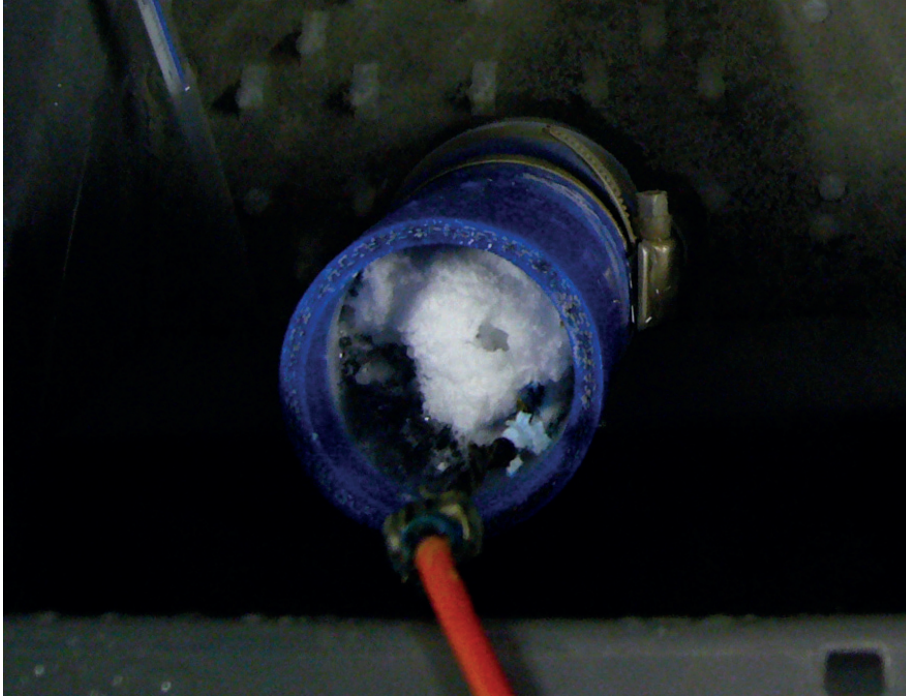


*Figure 3-5. Produced foam on top of anolyte solution*

### 3.4.3    Refreshment of anolyte/catholyte solution

As stated in previous section, although the advantage of applying LiOH as anolyte solution was proved due to its alkaline characteristics, the solution should be recharged with respect to the amount of $H^+$ ions produced at the anodic side. This regulation was also necessary to be performed for the catholyte solution, since the $OH^-$ ions produced at the cathodic side should have been consumed (according to Equation (3.4)). The produced amount of $H^+$ or $OH^-$ ions depends on the magnitude of applied electrical current during specific interval of experimental time which can be calculated with respect to Faraday's law of electrolysis presented in Equation (3.7) below:

$$I \cdot t = F \cdot z \cdot (\frac{m}{M})    \tag{3.7}$$

where,

*I*: Current (A)

*t*: Time (seconds)

*F*: Faraday number = 96485 (C/mol)

*M*: Molar weight of substance (g/mol)

*m*: mass of substance (g)

*z*: the valance number of ions

As shown in Table 3-3 and Table 3-4, in the course of Trial 4-9, electrical gradient is applied to the specimen through either constant potential or constant current. When constant potential was used the applied current through each specimen was monitored whilst when constant current was used the potential across each specimen was monitored. The main advantage of constant potential is to be able to test several specimens with one power supply whilst the use of a constant current makes is possible to predict the exact amount of electrical charge (Coulombs) through the specimen so as to be able to calculate the chemical dosage for recharging the ion solutions as well as the test duration for reaching the desired degree of leaching.

A constant current of 0.25 A for 24 hours would render the production of 0.22 M $H^+$ at the anode and the same amount of $OH^-$ at the cathode. This would require about 6 grams of LiOH to refresh the anolyte and about 18 grams of ammonium nitrate to refresh the catholyte solution.

Moreover, it was decided that solid salts could be directly added to the electrolyte solutions for recharging instead of refreshing the whole solution in order to facilitate the experimental procedure.

It should be noted that when recharging catholyte in order to consume possible precipitations inside catholyte solution, concentrated nitric acid (67% chemical quality) was also added to the catholyte in addition to solid ammonium nitrate.

### 3.4.4 Mechanical destructions

As it is illustrated in Figure 3-4 and presented in Section 3.4.2, cracking was detected in some specimens close to the cathodic side probably due to a combined effect of high osmotic pressure and constraining force by the clamp for tightening the sealant. In order to prevent this mechanical stress, only half of the area of specimen's curved surface was sealed.

It should be noted that the sealant according to the initial setup design was made of silicon rubber, but due to difficulties in disassembling the specimen after the experiment was replaced by asphalt tape.

As discussed in previous chapter aggressive effects of anolyte solution due to production of $H^+$ ions at the anode could cause destructions in the specimen as well. Although application of hydroxide salts as anolyte could improve the situation, to prevent direct contact between anode and the specimen, the anode was equipped with a plastic spacer.

### 3.4.5 Homogeneity of the leaching inside the specimen

Figure 3-6, illustrates the homogeneous distribution of electrical field inside the specimen when sealing the whole curved surface area of the specimen. However, it has been explained in previous section and also illustrated in Figure 3-4 in Section 3.4.2, that, if sealing the whole curved surface of the specimen, some cracking will occur close to the cathodic side. As illustrated in Figure 3-7, if sealing only half of the curved surface, the division of electrical field would not be homogenous through the specimen leading to inhomogeneous leaching in different levels of the specimen.

In order to find an approach to homogenizing the effect of the electrical gradients two trials was carried out. In Trial 10 the catholyte solution was refreshed using both ammonium nitrate and nitric acid whilst the pH level of catholyte solution was around 2-4 which implies acidic characteristics in catholyte solution causing coupled effect of electrical migration and acid dissolution on the unsealed surfaces of the specimen. However, although in this approach the degree of leaching at the bottom of specimen can be improved, the high concentration gradient of the electrical field in the upper

half part of the specimen (close to the anode), may cause possible degradation of C-S-H gel.

In experiment 11 the specimen was turned longitudinally halfway of the experiment. The halfway of experimental time is judged according to the leached amount of calcium ions from the specimen. It should be noted that in this experiment the pH level was well maintained around 7-9.

The setup parameters of Trial 10 and 11 are presented in Table 3-5.
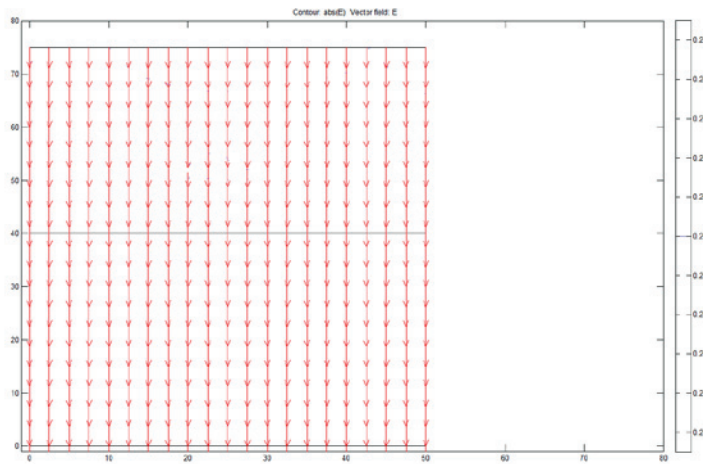


*Figure 3-6. Electrical current inside the specimen sealing whole curved surface area of the specimen*
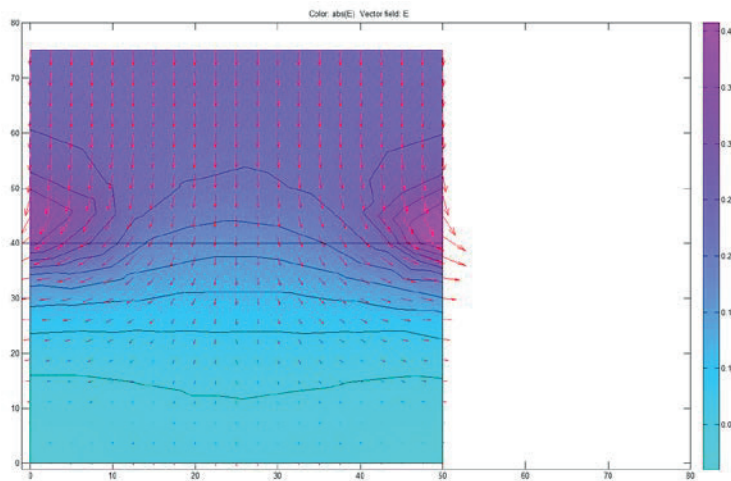


*Figure 3-7. Electrical current inside the specimen sealing almost half of specimen's curved surface area*

*Table 3-5. Set up parameters applied in the course of trials*

| Trial number | Anolyte | Catholyte | Current/ potential | Comment |
|---|---|---|---|---|
| 10 | 2M LiOH with addition of LiOH in powder form | 0.3 M $NH_4NO_3$ with an addition of solid $NH_4NO_3$ and Nitric acid with a pH level around 2-4 | 0.25 constant current | _ |
| 11 | 2M LiOH with addition of LiOH in powder form | 0.3 M $NH_4NO_3$ with an addition of nitric acid and maintained pH around 7-9 | 0.25 A constant | The specimen was turned halfway of the experimental time |

## 3.5    Final design-setup

As shown in Table 3-6, several parameters of the initial set-up design were improved based on the results from the course of several experimental trials. The final design set-up is illustrated in Figure 3-8. Figure 3-9, presents the course of reactions taking place in the system when implementing the final setup design.
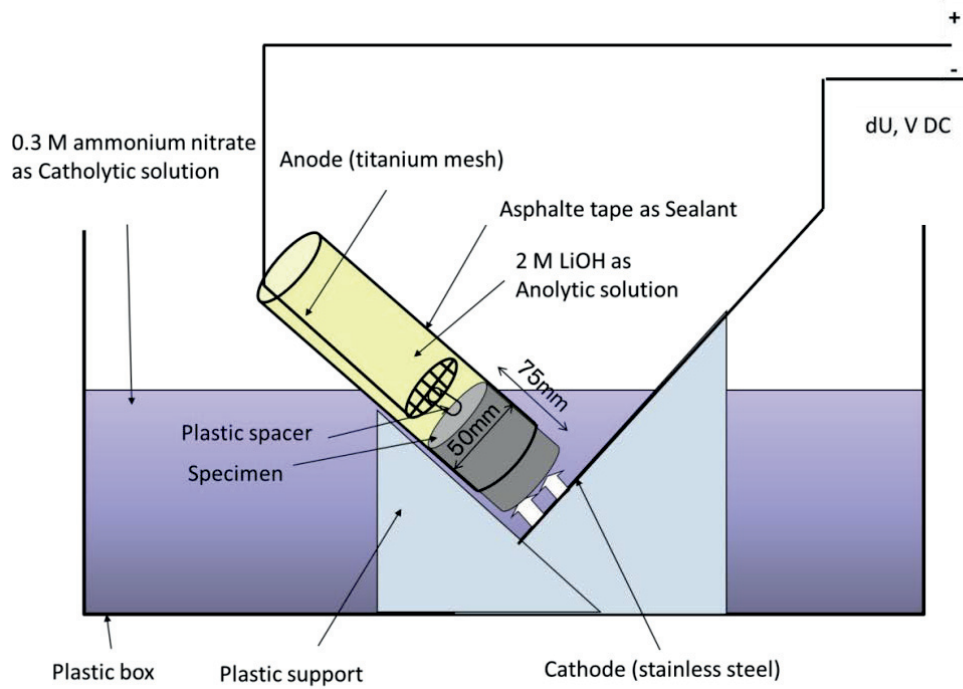
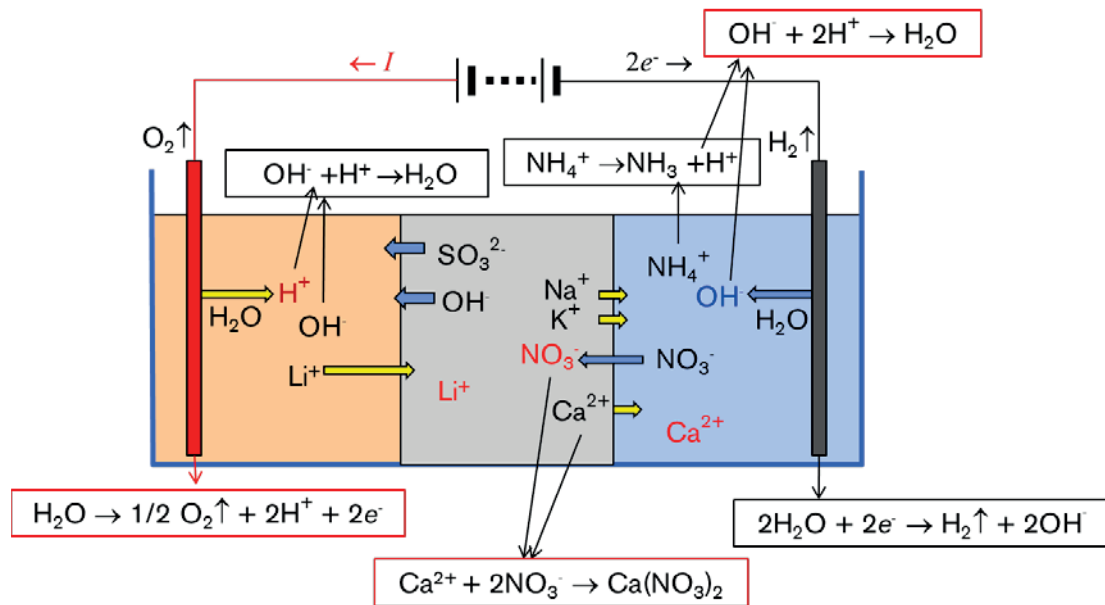*Figure 3-8. Final setup design of electrochemical migration method*



*Figure 3-9. The reactions taking place in the system implying final setup design of electrochemical migration method*

38

*Table 3-6. Refined parameters in final design of the electrochemical migration method*

| Parameter | | Modifications |
|---|---|---|
| **Catholyte solution** | **Type/Concentration** | Ammonium nitrate with an initial concentration of 0.3 M in a large volume (12-15 liters) is suitable as catholyte to leach out the calcium ions and also to send nitrate ions into the specimen to favor dissolution of Portlandite. |
| | **Refreshment** | The catholyte solution must be recharged with additional ammonium nitrate and nitric acid to neutralize the cathode-released OH$^-$ and maintain the pH value $< 9$ in the catholyte. The refreshment should be with respect to produced amount of OH$^-$ ions |
| **Anolyte solution** | **Type/concentration** | Lithium hydroxide with an initial concentration of 2 M in a relatively small volume (about 300 ml) is suitable as anolyte for compensating the cations and neutralizing the anode-released H$^+$ under certain test duration. |
| | **Refreshment** | The anolyte solution must be recharged with additional lithium hydroxide during the entire test period to maintain the pH $> 14$ in the anolyte. The refreshment should be with respect to produced amount of H$^+$ ions. |
| **Applied electrical feild** | | Constant current (250 mA for $\phi$50 mm cement paste specimen) |
| **Set-up design** | **Sealant** | In order to prevent the mechanical stresses causing cracking in the bottom of specimen, only half of the area of specimen's curved surface was sealed. |
| | | Silicon rubber is changed to asphalt tape due to difficulties in disassembling the specimen after the experiment as well as its high costs |
| | **Anode** | To prevent direct contact between anode and the specimen, the anode is equipped with a plastic spacer |
| | **layout of the specimen** | The specimen is turned longitudinally halfway of the experimental time |

## 3.6 Accelerations factor

As it is presented in Equation (3.8), applying Fick's second law it is possible to account for the diffusion process in a semi-infinite medium and eventually determine the mass of an element j, $m_{ji}$, leached during time interval $\Delta t_i$, having $D_{xj}$ as diffusion coefficient, from a medium where its concentration is $C_{1j}$, towards the leachate where its concentration is zero [27].

$$\sum m_{ij} = 2 \cdot C_{1j} \cdot S \cdot \phi \cdot \sqrt{D_{xj} \cdot \sum \Delta t_i \Big/ \pi} \tag{3.8}$$

where,

$S$: Surface area in contact with leachate

$\phi$: Porosity

It should be noted that the $m_{ji}$ should be expressed in terms of normalized leached fractions, $E_{qlix}$, against specimen's size [27], as expressed by Equation (3.9).

$$E_{qlix} = \frac{\sum m_{ij}}{M_{0j}} \cdot \frac{V}{S} \tag{3.9}$$

where,

$M_{oj}$: Total initial quantity of j in the sample

$V$: Sample volume

Figure 3-10, presents the normalized leached fractions versus the square root of time according to Equation (3.9) and with respect to the leaching results with implement of final set-up design, compared with experimental immersion results at pH 4.5, presented by Revertegat et al. [27] as well as the experimental results using ammonium nitrate presented by Heukamp et al. [21]. From the curves in Figure 3-10 it can be seen that the leaching rate (slope of the curve) by the electrochemical migration method is significantly larger than the other methods. An acceleration factor about 600 can be calculated for the migration method presented in this study by

40

comparing the leaching rate with the immersion test at pH 4.5 if we assume that the latter is close to the natural leaching.
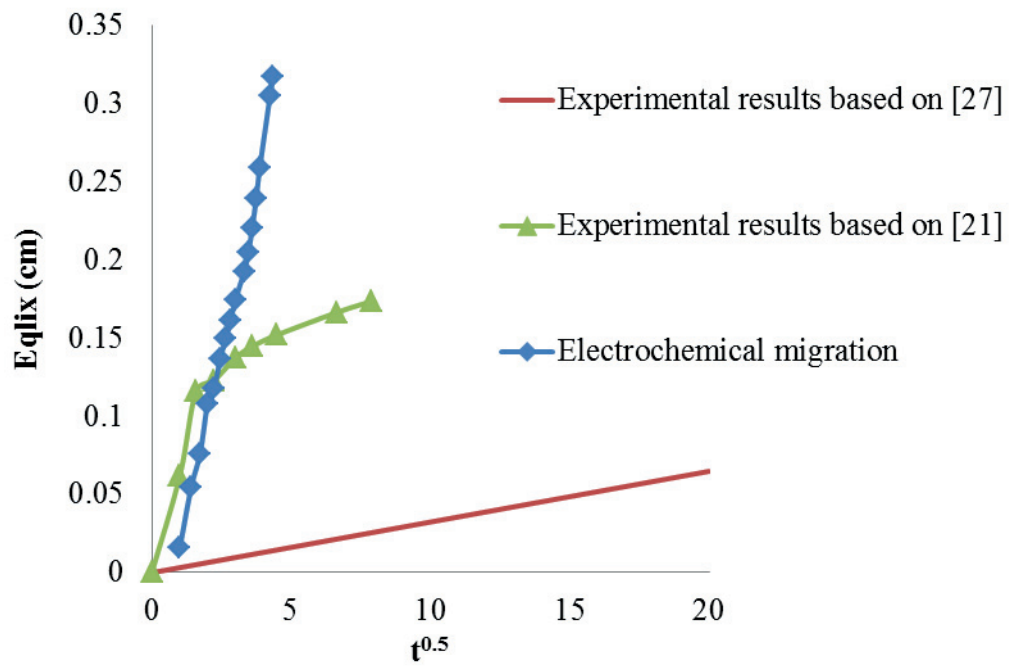


*Figure* **3-10**. *Normalized leached fraction of calcium as a function of square root of time based on the results from Trial 10 and the data in* **[21, 27]**

# 4 Other methods accelerating decalcification

In order to demonstrate the effectiveness of the electrochemical acceleration method for leaching of calcium from cementitious specimens and also in order to produce a data base regarding the chemical and mineralogical properties of aged cementitious materials, several acceleration methods reported in literature were performed in this study. As the rate of leaching would increase using smaller sample sizes most of the tests were performed using powder samples. In this section a description about these acceleration test methods and the experimental approach to perform them is presented.

The test specimens used in all of the tests were produced as explained in Section 3.1.

## 4.1    pH stat test method

The pH-stat method was designed enabling the effect of the pH and sample size for acceleration. The experimental procedure was based on a method presented by Gustafson et al. [33]. In this method a constant pH level lower than that of the natural situation was applied to powdered samples through frequent acidification. The added volume of acid and the changes in temperature for an experiment aiming for pH=8, is presented in Figure 4-1.

A powder size of about 0.1 mm (0.075-0.125) was used in the pH stat test. In order to prepare the powder, thin slices were cut from the cylindrical specimen after more than 6 months moist curing. The slices were crushed and ground under wet conditions in order to reduce the risk of carbonation. 12 gr of powder was mixed with 50 ml of Milli-Q water and 6.5 ml of concentrated Nitric acid (67% chemical quality) was added to the mix to reach to the initial pH of 8. Automated Potentiometric Titration method using a Metrohm 836 Titrando titrator was employed in order to perform the test. The titrator was equipped with a magnetic stirrer as well as two dosimeters. The pH electrode with built in thermometer was used to monitor the pH value in the solution. The electrode was calibrated with standard buffer solutions before use. The titration procedure was controlled by TIAMO software. Nitric acid of 3.7 M was used to maintain the natural pH value of 8. The experiment duration was set to 24 hours because stable equilibrium was observed under this time period. After termination of the experiment the solid part was separated from liquid through vacuum filtration.

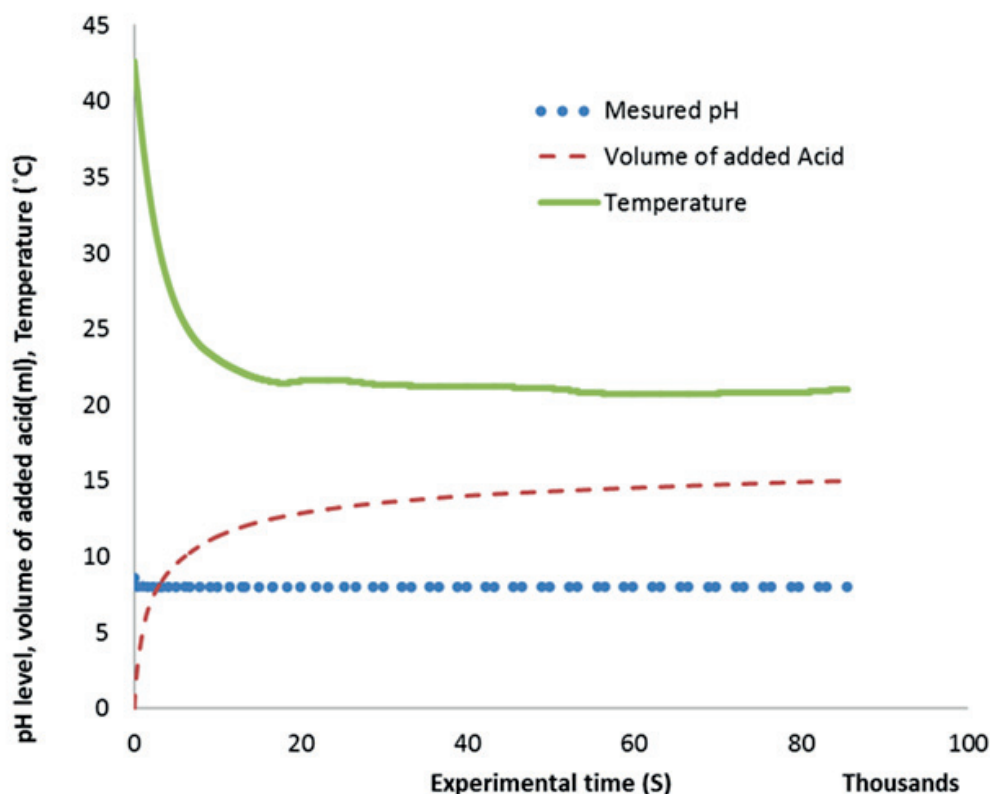The filtrate was vacuum dried in order to be analyzed regarding its chemical and mineralogical properties.



*Figure 4-1. Temperature change and the added amount of acid to the cementitious sample in pH stat test for pH level 8*

## 4.2    Flash column test

The effect of large surface area using powder samples can be enhanced using an advective flow passing through the particles. In the column test, a 110 ml glass chromatography column with a fritted disc equipped with a PTFE plug to control flow rate was used. The same powder size as in pH stat test was used. The sample was filled into the column on the fritted disc and subjected to upward water flow with a flow rate of less than 2.5 ml/s. The column was connected to a reservoir with the capacity of 5 litres through PVC tubes from both sides. Demineralized water was used as circulating solution in the system. The pH value of the solution was manually monitored. When the pH value in the circulating solution was around 12, the whole solution in the reservoir was refreshed. The experiment was continued until the pH

value in the solution became constantly low (about 8). Figure 4-2 illustrates the experimental set up of the flash column leaching test.

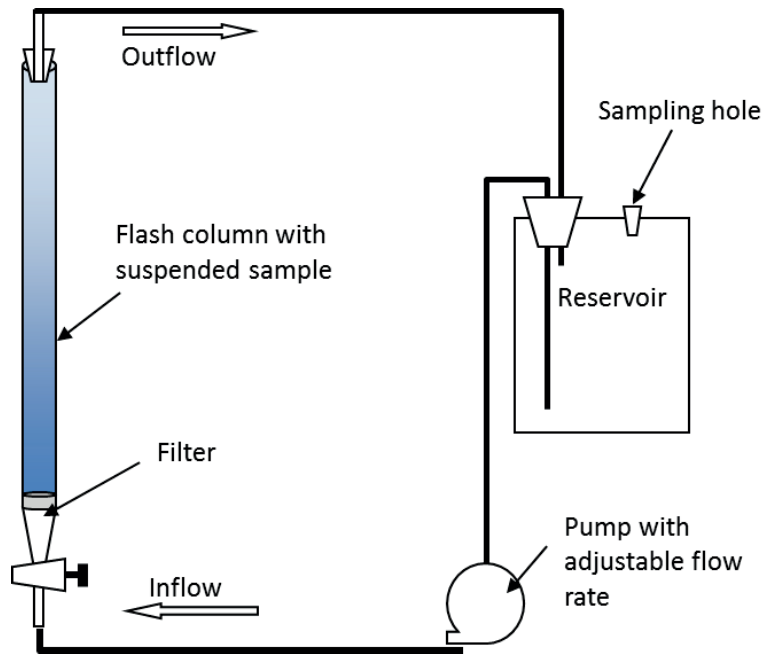A sililar set-up design can be found in an study presented by Pfingsten and Shiotsuki [34].



*Figure 4-2. Experimental setup of the flash column test*

## 4.3    Carde's method

It has been presented in Section 2.4 that  an effective accelerated decalcification in cementitious specimens was achieved with application of ammonium nitrate solution as presented by Carde [20]. In order to compare the properties of the aged specimens by the electrochemical migration test with those by Carde and Francois [15], the test with immersion of paste specimens in concentrated ammonium nitrate solution was performed. Thin cylinders (Ø10 mm) of paste specimens with the same mix design and casting procedure as presented in Section 3.1, were produced and cured for 1 year. The cylinders were cut into small pieces with a size of Ø10×60 mm and immersed in 1 liter of  6 M ammonium nitrate solution in a vacuumed desiccator container (the container was vacuumed to prevent carbonation). The content was stirred during the experimental time (using magnetic stirrer) to homogenize the

effects. The test was carried out for 45 days in order to reach the quasi steady state as presented by Heukapm [21].

# 5 Chemical and Mineralogical Analysis

In this chapter the investigations regarding the chemical and mineralogical properties of the specimen in the course of the acceleration test as well as the homogeneity of the properties in different parts of the specimen is presented.

The mineralogical characteristics of the samples tested in Trial 10 are also presented in this chapter.

Furthermore, the solution analysis results are presented and finally the chemical and mineralogical properties of the samples aged with application of test methods presented in Section 4 are presented.

## 5.1     Instrumental analysis

### 5.1.1     XRD

X-Ray Diffraction (XRD) analysis provides qualitative and quantitative information regarding crystalline phases in materials, specifically the arrangement of atoms within those phases. This method is developed based on uniqueness of diffraction pattern from each crystalline phase. For powder diffraction analysis the solid sample should be grinded in to fine powder. The sample holder is thin-walled glass. A spectrum based on relative intensity and the position in line ($\theta$ or $2\theta$) would be the result. The specific peak lines within the spectrum would be compared with databases to find a match. In this work a Siemens D5000 powder diffractometer, equipped with Göbel mirror is used.

### 5.1.2     XRF

X-Ray Fluorescence spectroscopy (XRF) analysis is a fast and non-destructive method used for elemental analysis ranging from silicon to uranium. The technique can be used for determining element concentrations in a sample over the range between parts per trillion (ppt) and % quantities. The analysis is based on differences in either wavelength or energy of the elements being analyzed. In this study the results from the XRF analysis are presented as a function of the changes of calcium to silica ratio of the treated specimens compared to the original ratio i.e.

$$\frac{\left(\frac{Ca}{Si}\right)_{Treated}}{\left(\frac{Ca}{Si}\right)_{Re\,ference}}$$ . The reason for using this ratio is that by the time of performing

these analyses, due to problems with instrumental calibration the quantified amount of

each element in samples was not available. However $\frac{\left(\frac{Ca}{Si}\right)_{Treated}}{\left(\frac{Ca}{Si}\right)_{Re\,ference}}$ was obtained

with respect to peak area of each element. The used spectrometer is built of a W-anode X-ray tube and a Mo secondary target as described by Boman [35]. It is a three-axial geometry spectrometer with a Si (Li) detector of 80 mm2 active area, and a resolution of 175 eV FWHM for Mn-Kα X-rays. Spectrum acquisition time was 1000 s at a tube voltage of 55 kV and current of 15-25 mA.

### 5.1.3    SEM and EDAX

Scanning Electron Microscopy (SEM) is a method to produce high magnified images by scanning the sample with a focused beam of electrons. The interaction between the electrons and the sample produces various detectable signals containing information regarding sample's surface topography and composition. The image detection can be in low and high vacuum conditions and with environmental SEM instruments wet samples can be analyzed as well. The SEM instrument can be equipped with the Energy Dispersive X-ray spectroscopy (EDX) in order to detect the elements through the X-rays produced by the interaction between the electrons and the sample. In this work a FEI Quanta ESEM 200 equipped with a Field Emission Gun is used. It has an Oxford Inca EDX system, used for both quantifying elemental concentration.

### 5.1.4    IC

Ion Chromatography (IC) is a method to quantify the content of charged substances in a solution. The sample is typically injected in to the instrument manually or with an auto-sampler. The ions of interest are detected typically by conductivity or UV/visible light absorbance. An IONEX (ICS 900) Ion Chromatograph was used in this syudy.

## 5.2 Mineralogical properties of the aged specimen after Trial 11

As it was explained in Section 3.4.5, to homogenize the effect of electrical gradient inside the specimen, the specimen should be turned half way of experimental time. In order to compare the homogeneity of the leaching, the same experimental parameters as in Trial 11, is applied to 6 specimens in parallel, however the experimental time and the turning approach differs between the specimens. The specific experimental set-up parameters regarding Specimen 1-6 is presented in Figure 5-1and Table 5-1. Figure 5-2 illustrates the observable changes inside the specimens in the course of acceleration test method. It can be seen that a layered structure exist in the cross-section of the specimen, a greyish circle in the middle surrounded by a thin black ring and a light brownish circle. The greyish circle in the middle of the specimen is getting smaller through time after passing a higher amount of electrical charge. Comparing specimen 4 & 6, it can be seen that after turning the specimen the observable layered structure in the cross section of the specimen became homogenized all over the specimen.
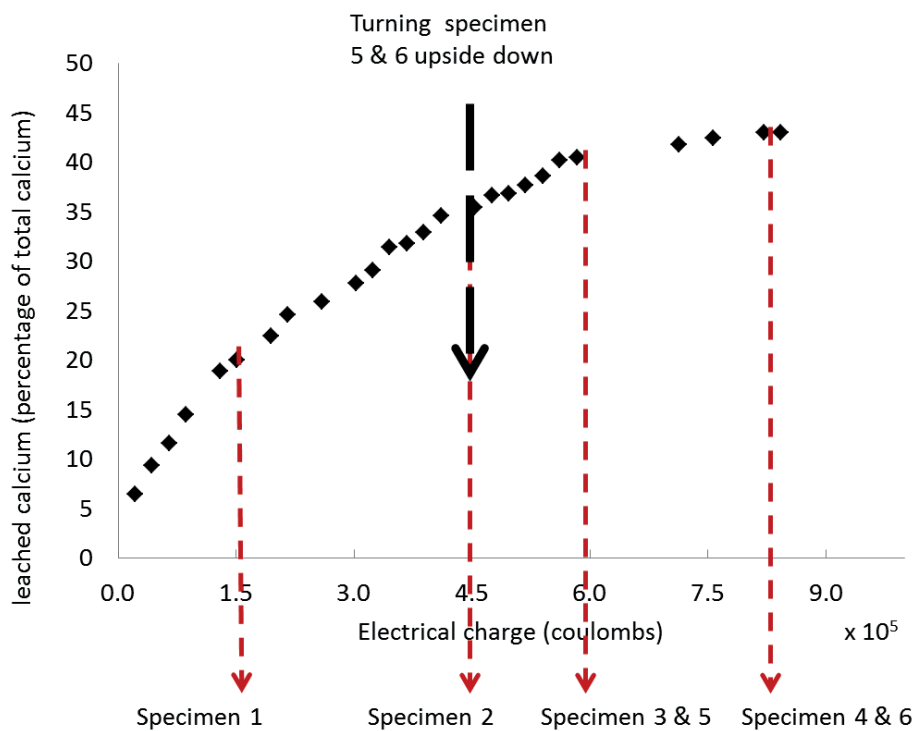


*Figure 5-1. The timeline of termination of the experiment for Specimen 1-6*

*Table **5**-1. Experimental details regarding Specimen 1-6*

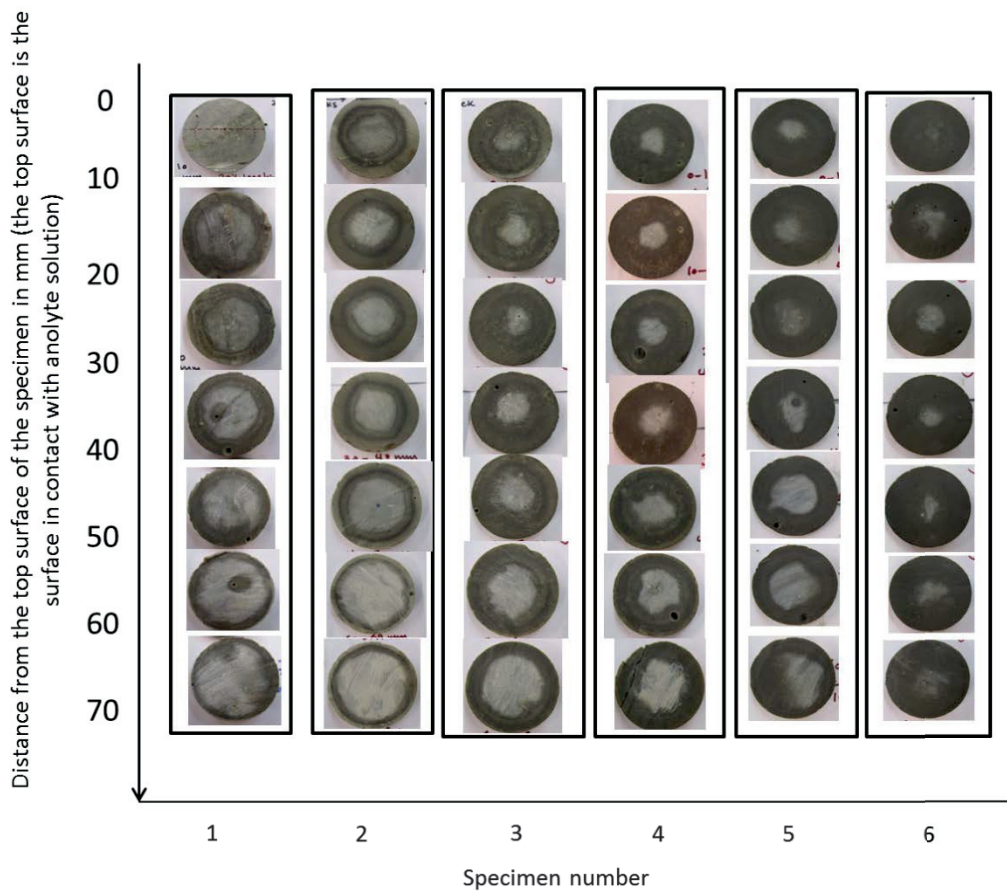| Specimen Number | Applied electrical charge | Experimental time | Comment | Total Leaching of Calcium (% of total calcium content) |
|---|---|---|---|---|
| 1 | $1.51 \times 10^5$ | 168 | the specimen is <u>not</u> | 20% |
| 2 | $4.53 \times 10^5$ | 504 | <u>turned</u> during the | 30% |
| 3 | $5.83 \times 10^5$ | 648 | experimental time | 40% |
| 4 | $8.42 \times 10^5$ | 936 | | 41% |
| 5 | $5.83 \times 10^5$ | 648 | the specimen is turned | 36% |
| 6 | $8.42 \times 10^5$ | 936 | upside down after 456 hours | 43% |



*Figure 5-2. The observable changes inside the specimen in the course of the acceleration test*

### 5.2.1  X-Ray analysis results

In order to account for the mineralogical properties of different layers observed in the cross section of treated specimens, XRD and XRF analysis were carried out.

Figure 5-3 illustrates the sample numbering. It is shown that the outer brownish layer is numbered 1, the thin black circle is 2 (the thin black circle was not observable in the specimen turned halfway of the experiment after passed $8.42 \times 10^5$ Coulombs of electrical charge) and the greyish area in the middle is numbered 3.

Three different depth levels, 0-10 mm, 30-40 mm and 50-60 mm (with respect to the distance from the anodic side), and two magnitude of electrical charge, $1.5 \times 10^5$ and $8.42 \times 10^5$ Coulombs, were chosen.

The samples were grinded into powder under wet condition with ethanol and vacuum dried before the analysis. For XRD analysis 0.5 grams of powder and for XRF analysis 0.1 grams of powder is used.

The XRD results are presented in Figure 5-4. The results indicate that the outer brownish layer (1) as well the blackish thin circle zone (2) is not containing Portlandite. However, the grayish middle section (3) contains Portlandite although the peaks are slightly lowered.

Moreover, the XRF analysis results are presented in Figure 5-5. As mentioned in Section 5.1.2, the results from the XRF analysis are presented as a function of the changes of calcium to silica ratio of the treated specimens compared to the original ratio i.e. $\dfrac{\left.\dfrac{Ca}{Si}\right|_{Treated}}{\left.\dfrac{Ca}{Si}\right|_{Re ference}}$ . According to Table 3-2 presented in Section 3.3, the calcium silica ratio of an untreated (specimen) is 2.54 and if considering only Portlandite to be leached out from the specimen after treatment this value would be 1.5, which gives $\dfrac{\left.\dfrac{Ca}{Si}\right|_{Treated}}{\left.\dfrac{Ca}{Si}\right|_{Re ference}} = 0.59$ .

**1.5×10$^5$ Couloumbs electrical charge**

| 1.a 2.a 3.a | 1.a 2.a 3.a | 1.a 2.a 3.a |
| 0-10 mm | 30-40 mm | 50-60 mm |

**8.42×10$^5$ Coulombs electrical charge (turning the specimen halftime of experimental)**

| 1.b 3.b | 1.b 3.b | 1.b 3.b |
| 0-10 mm | 30-40 mm | 50-60 mm |

**8.42×10$^5$ Coulombs electrical charge (the specimen IS NOT turned)**

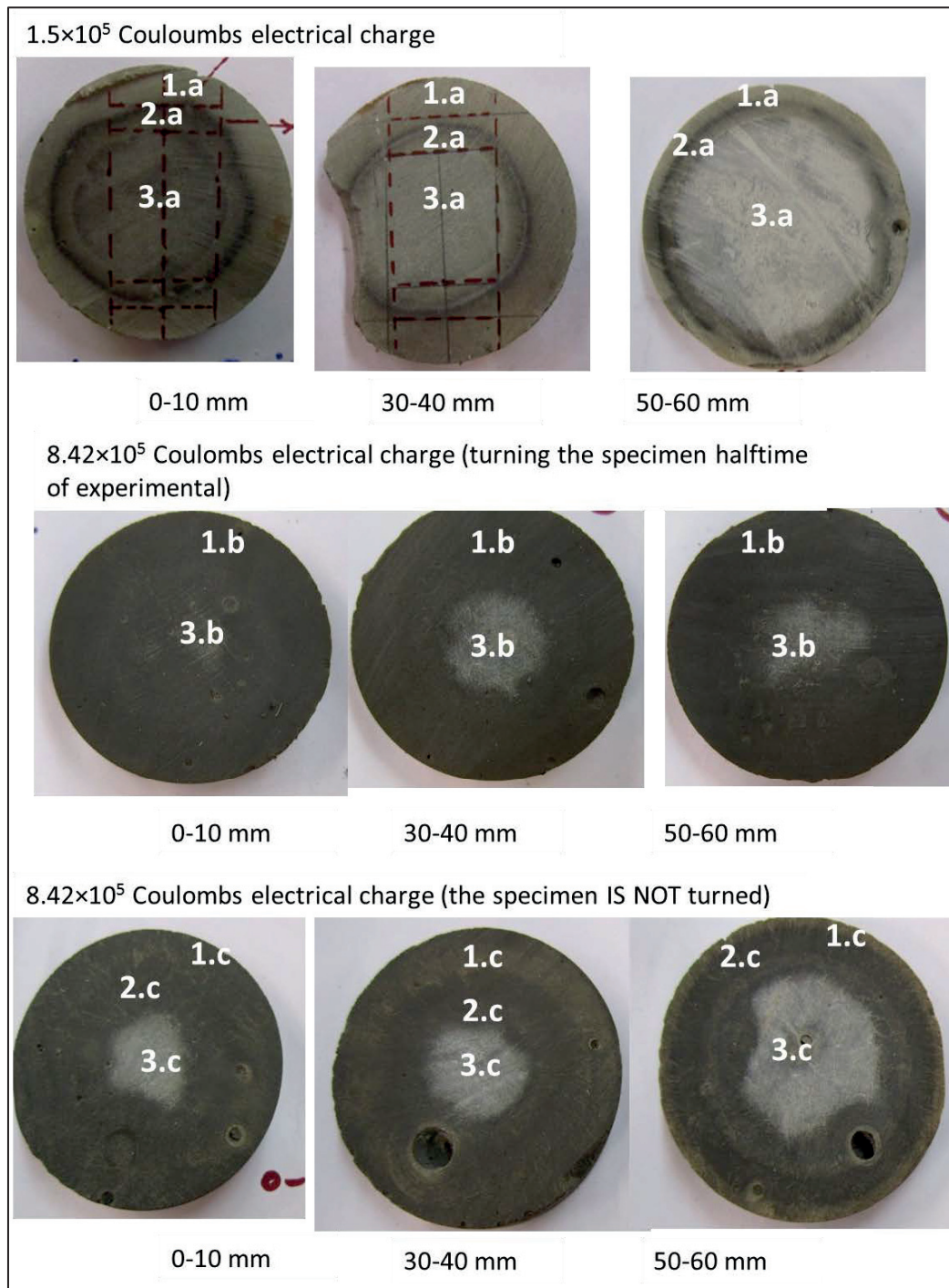| 1.c 2.c 3.c | 1.c 2.c 3.c | 2.c 1.c 3.c |
| 0-10 mm | 30-40 mm | 50-60 mm |

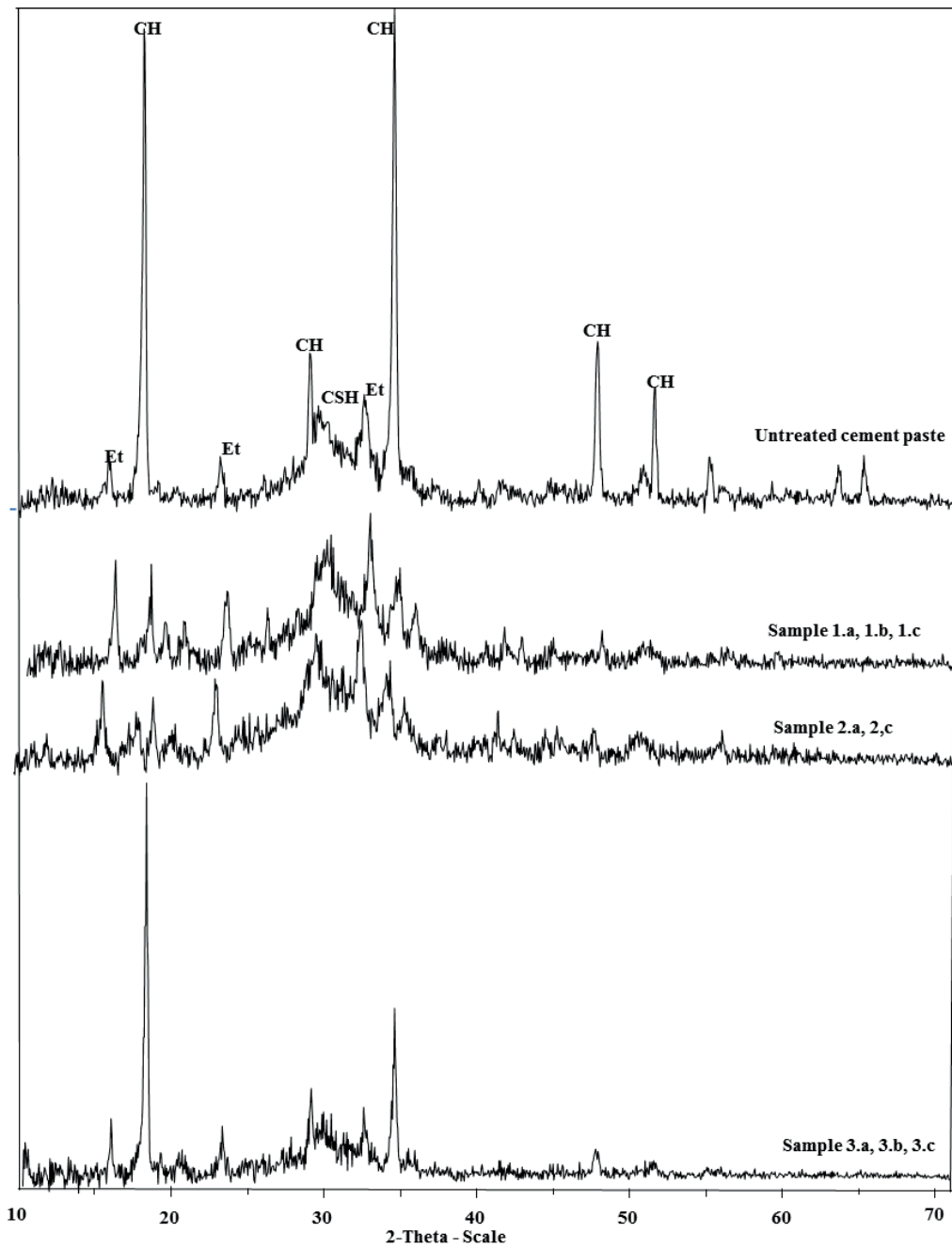*Figure 5-3. Sample numbering regarding X-Ray analysis*

*Figure 5-4. XRD results regarding the layered structure in the cross section of treated specimens*

As presented in Figure 5-5, the grayish middle part of the sample is showing the same Ca/Si as the reference. However the outer brownish layer and the middle black circle zone are showing lower Ca/Si. In the case that the specimen was turned halfway of the experiment the Ca/Si of the outer layer is close to 0.6 which is an indication of complete leaching of Portlandite, but if the specimen was not turned the Ca/Si ratio of

57

the outer layer is lower than 0.6 in the upper part of the specimen, which implies possible decalcification of C-S-H gel.

It should be noted that with respect to X-Ray results only in the case of turning the specimen halfway of the experiment the homogenized leaching of total Portlandite content can be obtained inside the specimen, which is in accordance with the discussion presented in Section 3.4.4 and 3.4.5. (The leached amount of calcium is about 95% of Total Portlandite content and the remaining 5% should be the small grayish layer remained in the middle of the specimen)
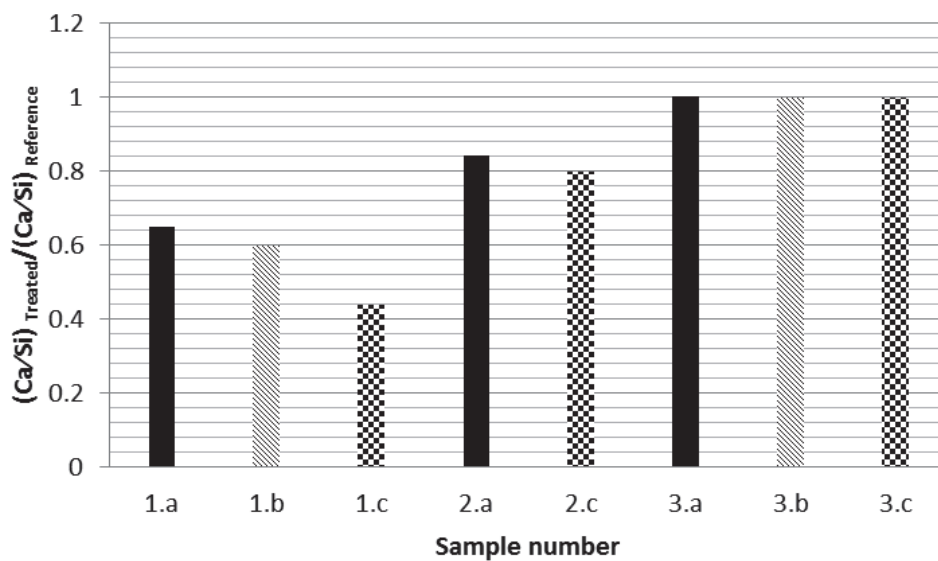


*Figure 5-5. XRF analysis comparing the layered structure of the treated specimens*

### 5.2.2 SEM/EDAX analysis results

In order to analyze the microscopic topography and composition of treated specimens, SEM analyses are performed. Figure 5-6, illustrates the sample used in SEM analysis and the Sample numbering. Each layer named 1-3 are cut in to cubic samples and vacuum dried before the analysis. The specimen chosen for the analysis is treated with 8.42E05 coulombs of electrical charge and it is not turned halfway of the experiment. The reason of choosing this specimen is that the layered structure in cross section of the specimen is quite obvious specifically in the upper part of the specimen. The sample is taken from 10-20 mm distance from the anodic side of the specimen.
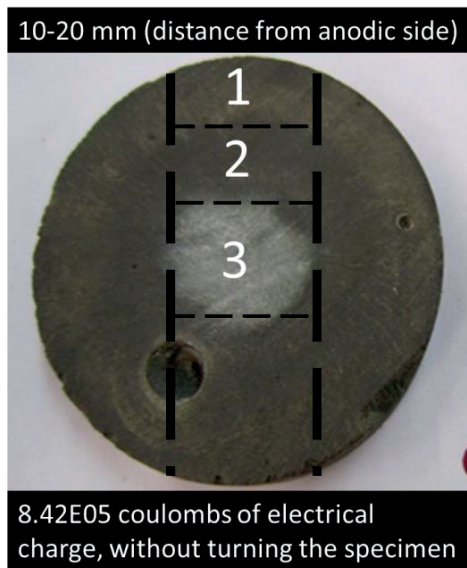
*Figure 5-6. Sample numbering for SEM analysis*

The SEM analyses of the untreated (reference) and the treated samples are presented in Figure 5-8 and Figure 5-8, respectively. As can be seen in the figures, the average Ca/Si in the treated sample decreases toward the curved surface of the specimen which is in agreement with the results from X-Ray analysis. The results indicate that the specimen became more porous towards its curved surface.

In general, there is a high deviation in Ca/Si ratio of layer 3, which indicates presence of both CH and C-S-H parts of the HCP (the same as in the reference sample), while the random point analysis in layer 1 and 2 shows similar Ca/Si ratio for all the points, which is due to leaching of the Portlandite content in these layers.

Moreover, the results from the point analysis shows that the Al and Fe content in the treated specimens is much lower than that in the reference sample which indicates possible decomposition of the phases containing those elements after treatment. The lighter color of layer 1 should be due to leaching of iron in this layer.

Another interesting point is the sulfur content in layer 2, which is higher compared to the other two layers as well as to the reference sample. A possible explanation is that the secondary precipitation of Ettringite took place in this layer which revealed the color of blackish circles. The blackish circle became thicker in the course of the experiment especially in the parts having lower leaching rate and it vanished through

59

time in the zones with higher leaching rate. This indicates that the precipitation of Ettringite is more significant in the parts with lower leaching rate of calcium and also is magnified when the leaching is not homogenized (Figure 5-2).

Reference sample
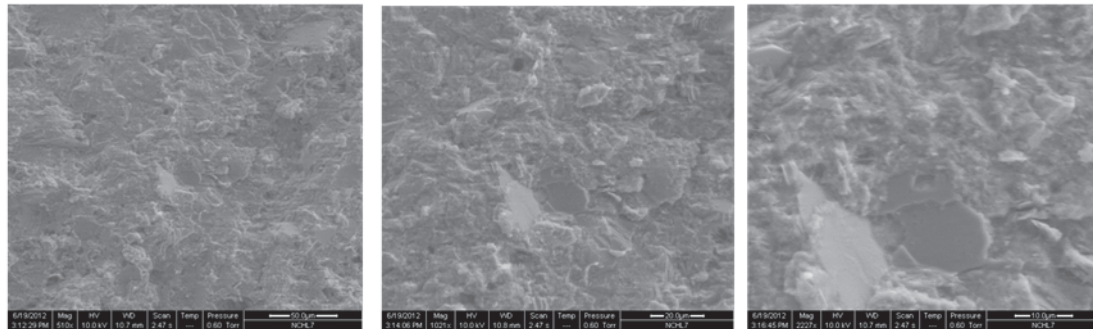


| Average Spectrum | In stats. | O | Na | Al | Si | S | K | Ca | Fe |
|---|---|---|---|---|---|---|---|---|---|
| Mean | | 44.56 | 0.20 | 3.65 | 6.95 | 0.33 | 2.00 | 33.94 | 8.37 |
| Std. deviation | | 12.39 | 0.04 | 1.84 | 1.95 | 0.10 | 0.93 | 10.63 | 2.54 |
| Max. | | 59.60 | 0.24 | 6.03 | 9.23 | 0.42 | 2.88 | 48.51 | 12.12 |
| Min. | | 24.40 | 0.15 | 1.96 | 4.39 | 0.17 | 0.80 | 20.64 | 4.31 |

*Figure 5-7. SEM/EDS analysis for the reference sample*

Layer 1        Layer 2        Layer 3

60 µm

| Spectrum | (Atomic%) | O | Na | Al | Si | S | K | Ca | Fe |
|---|---|---|---|---|---|---|---|---|---|
| Layer 1 | | 74.99 | 0.12 | 1.39 | 9.81 | 0.55 | 0.03 | 12.01 | 1.09 |
| Layer 2 | | 76.59 | 0.09 | 0.99 | 6.08 | 0.70 | 0.01 | 14.75 | 0.78 |
| Layer 3 | | 76.08 | 0.05 | 0.76 | 4.77 | 0.38 | 0.01 | 17.40 | 0.55 |

20 µm

| Average Spectrum | (Atomic%) | O | Na | Al | Si | S | K | Ca | Fe |
|---|---|---|---|---|---|---|---|---|---|
| Layer 1 | | 74.77 | 0.12 | 1.50 | 11.30 | 0.49 | 0.01 | 10.94 | 0.87 |
| Layer 2 | | 76.43 | 0.08 | 1.00 | 7.25 | 0.69 | 0.02 | 14.07 | 0.46 |
| Layer 3 | | 75.16 | 0.13 | 0.90 | 5.45 | 0.41 | 0.05 | 16.95 | 0.95 |

10 µm

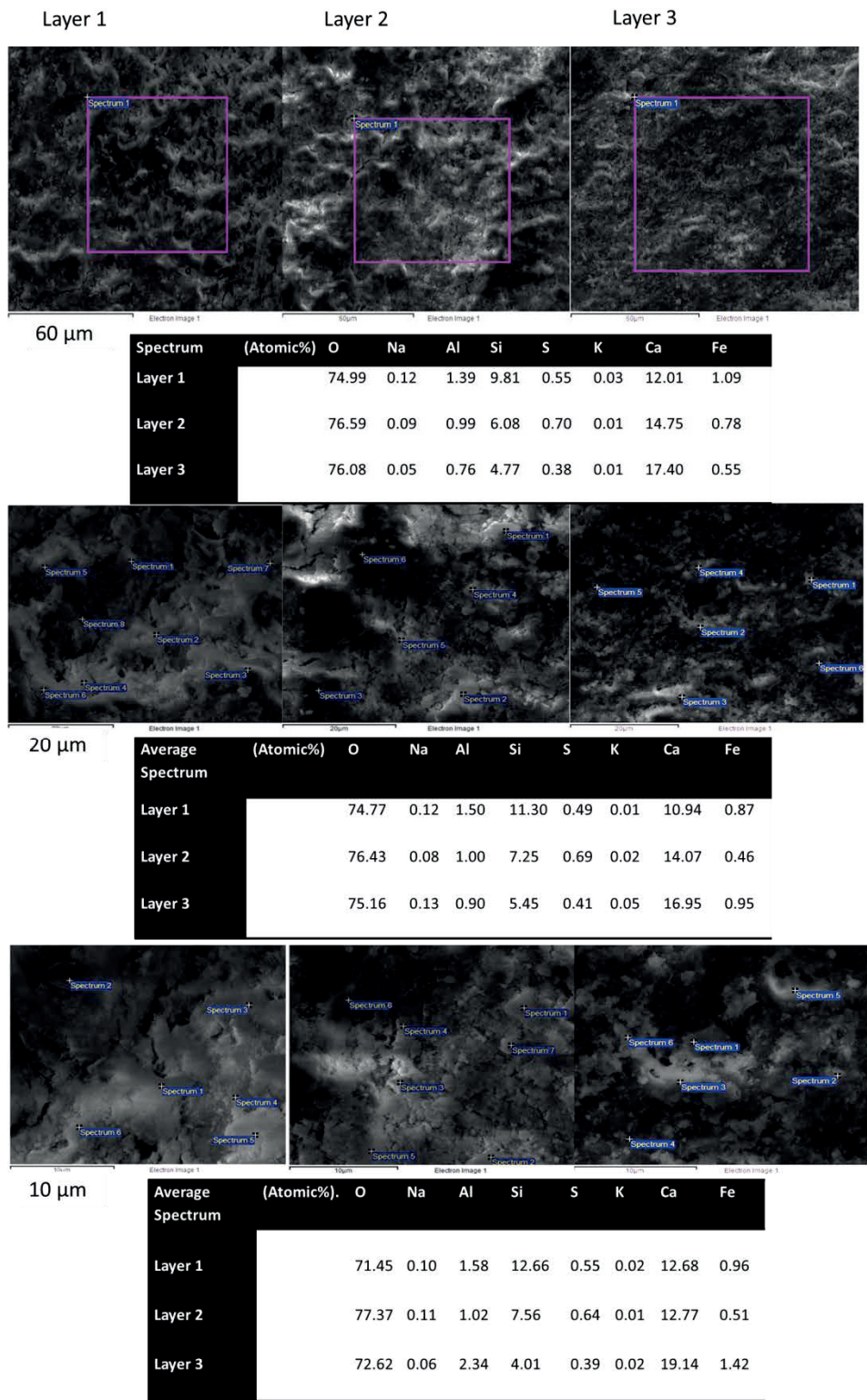| Average Spectrum | (Atomic%). | O | Na | Al | Si | S | K | Ca | Fe |
|---|---|---|---|---|---|---|---|---|---|
| Layer 1 | | 71.45 | 0.10 | 1.58 | 12.66 | 0.55 | 0.02 | 12.68 | 0.96 |
| Layer 2 | | 77.37 | 0.11 | 1.02 | 7.56 | 0.64 | 0.01 | 12.77 | 0.51 |
| Layer 3 | | 72.62 | 0.06 | 2.34 | 4.01 | 0.39 | 0.02 | 19.14 | 1.42 |

*Figure 5-8. SEM analysis comparing the microscopic topography and composition of the layered structure in the cross section of the treated specimens*

61

## 5.3 Mineralogical properties of the aged specimen after Trial 10

The mineralogical properties of the specimens produced in experiment 10 are presented in this section based on the results from X-Ray analysis.

Figure 5-9 illustrates the sample numberingregarding X-Ray analysis.

The XRD results are presented in Figure 5-10, indicating that the Portlandite peaks decreased to a large extent all over the specimen. Both Ettringite and C-S-H are detected in the samples close to both the anode and the curved surface of the specimen. The evidence of peaks for both Ettringite and C-S-H in samples 1-7 indicates that the migration method is more selective for Portlandite leaching. In order to confirm the repeatability of the method a repeatability test was performed with 4 specimens ageing in parallel and with implement of the same design setup as in Trial 10.

The results from XRF analysis indicate a strong decrease in Ca/Si ratio, following the depth from the anodic towards the cathodic side of the specimen as well as from the center towards the curved surface of the specimen, as shown in Figure 5-11. Some results from SEM analysis are shown in Figure 5-12, indicating a higher porosity in treated specimens compared with the untreated samples.
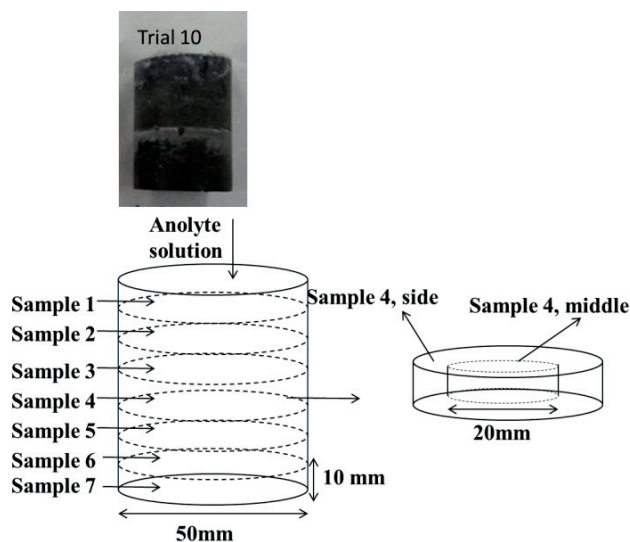


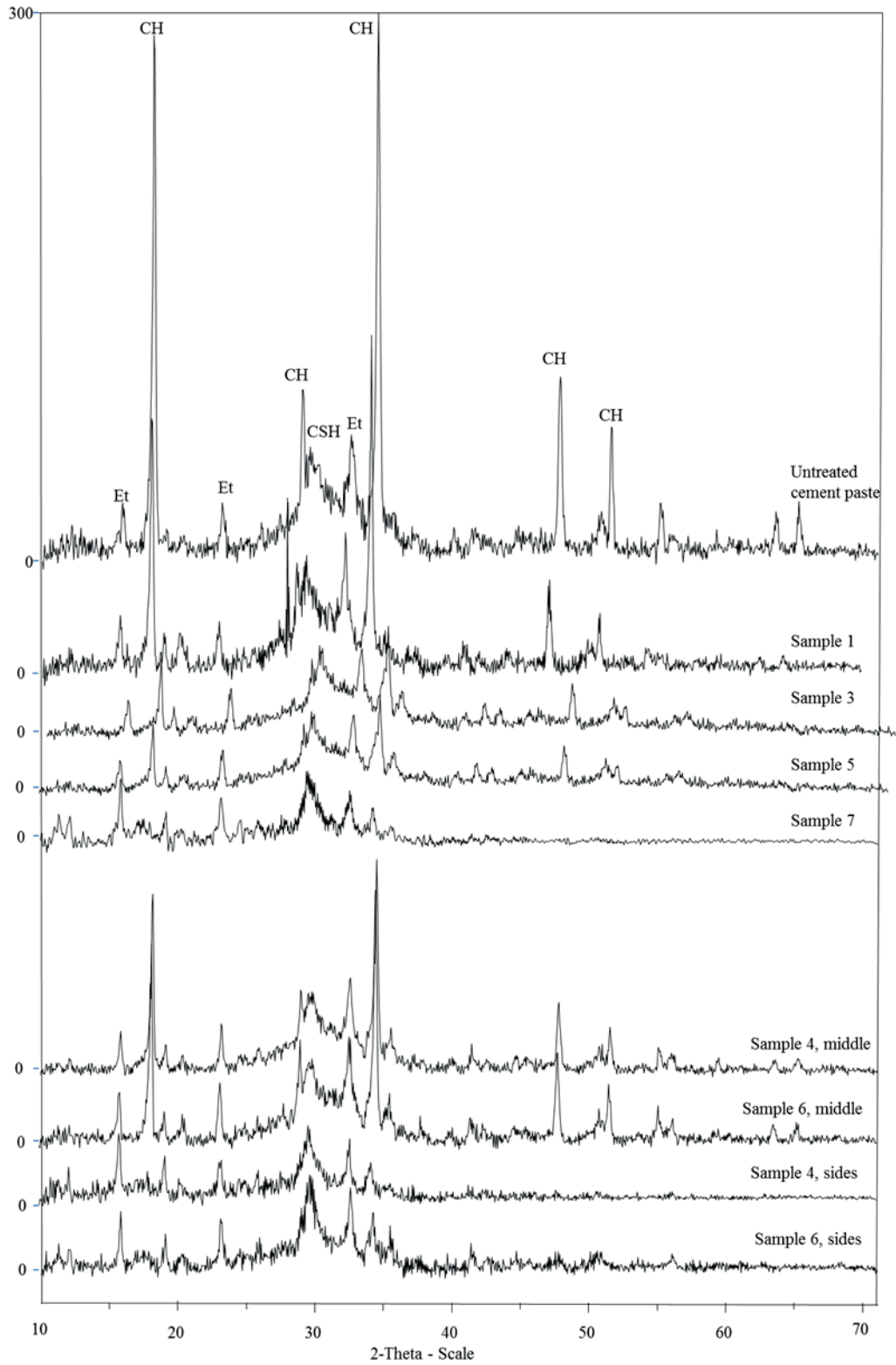*Figure 5-9. Sample numbering regarding X-Ray analysis in Trial 10*

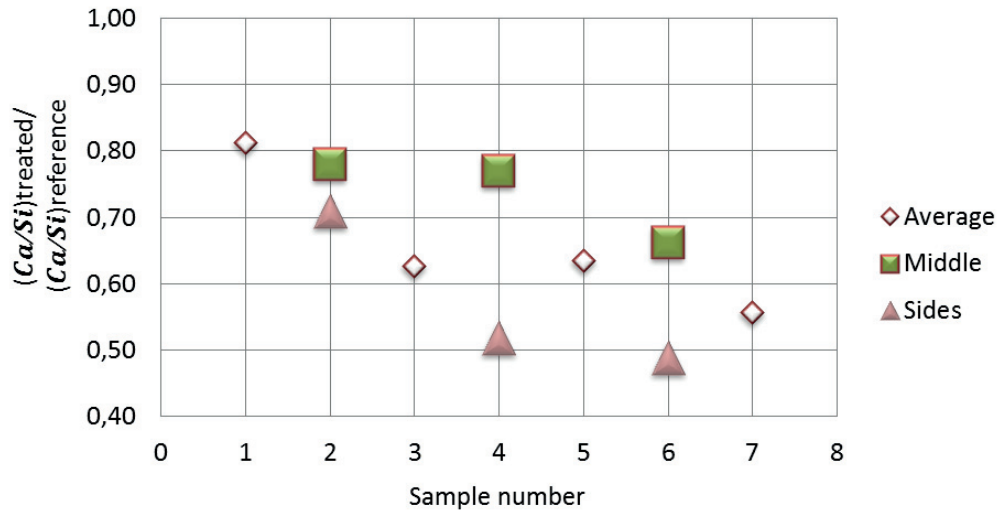*Figure 5-10. XRD results based on the aged samples in Trail 10*

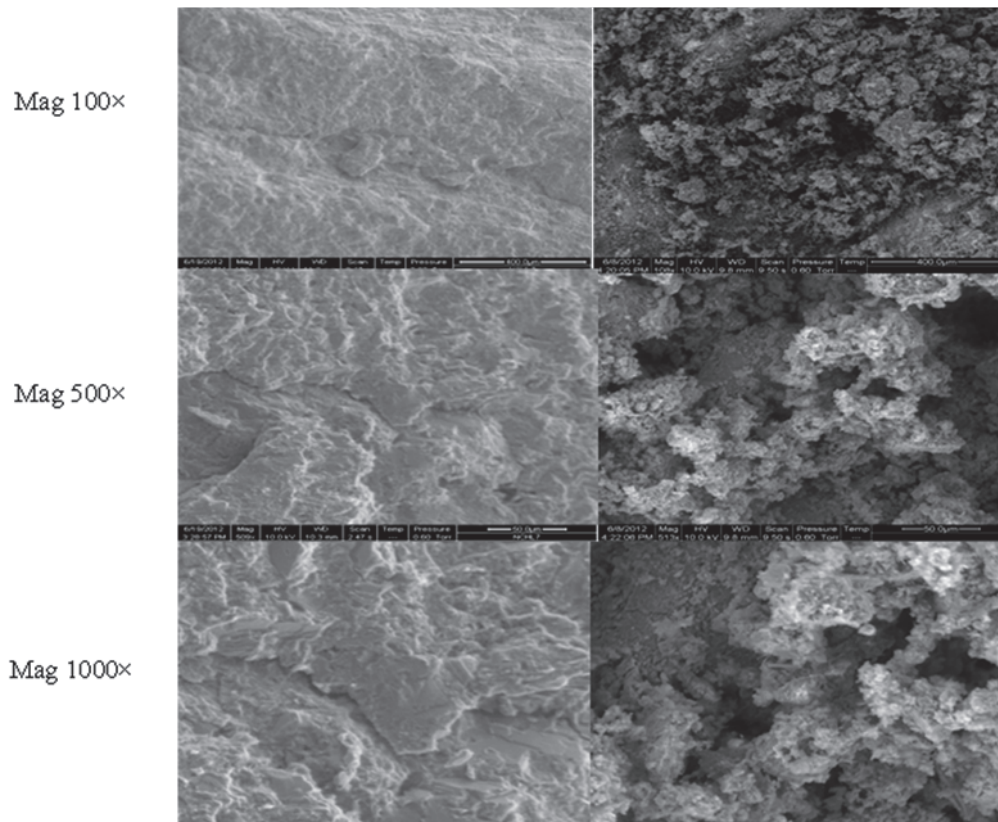*Figure 5-11. Results from XRF analysis presented based on*



*Figure **5-12**. Images from SEM analysis: comparison between untreated (left side) and treated specimens (right side)*

## 5.4 Solution analysis

The content of cations in the catholyte solution was measured through IC analysis. Figure 5-13 and Figure 5-14 present the IC results performed on the catholyte solutions from Trials 9 and 10. In Trial 10 the sodium and potassium are leached out from the specimen at the very beginning of the experiment and after that calcium leaching became dominant. Comparing the solution analysis results, it can be seen that potassium leaching rate is the same in both trials, whilst the calcium leaching rate is higher in Trial 10 in which lithium hydroxide was maintained in the anolyte solution, which is in agreement with the discussion presented in Section 3.4.2. Compared with Trial 9 in which NaOH was added to the anolyte as refreshing agent especially after 400 hours, the enhanced leaching of $Ca^{2+}$ in Trial 10 might be linked with the hydrated size of Li ion as discussed in Section 3.4.2.
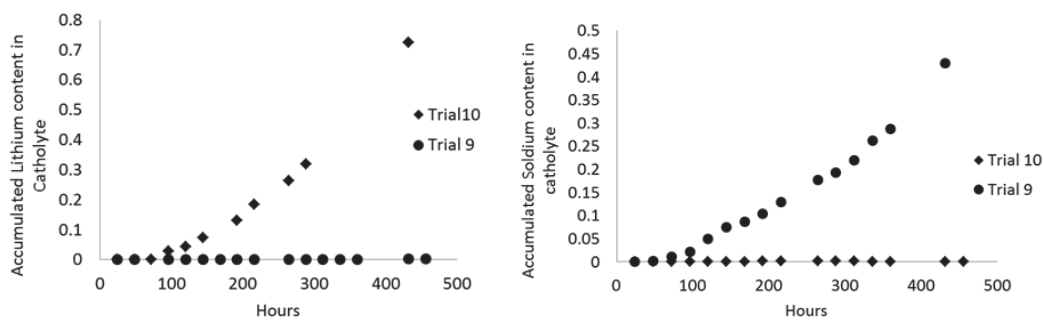


*Figure 5-13. Accumulated lithium (left side) and sodium (right side) contents in the catholyte solution in Trials 9 and 10*
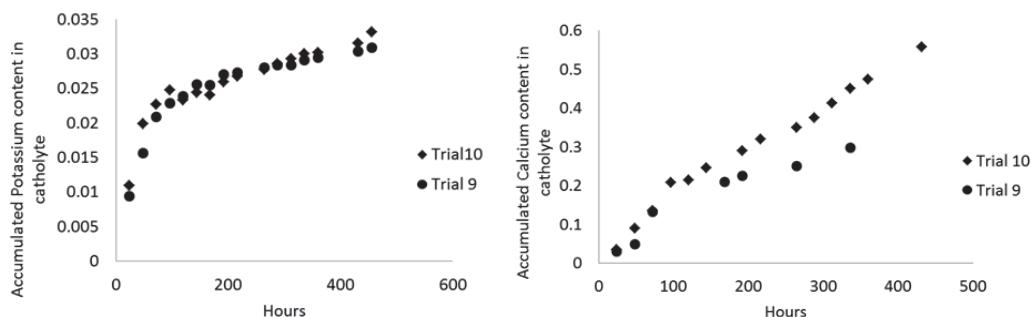


*Figure 5-14. Accumulated potassium (left side) and calcium (right side) contents in the catholyte solution in Trials 9 and 10*

A scenario can be depicted in which the dissolved Ca2+ ions can more easily migrate out through the pores than the Li+ ions while the Na+ ions may compete with the Ca2+ ions for carrying the imposed current, resulting in less calcium leaching. It should be noted that the leached amount of sodium in Trial 10 is much lower compared to that of calcium and as a results the values are close to zero as presented in Figure 5 13.

## 5.5 Comparison of the samples aged with different acceleration methods

In this section the chemical and mineralogical analysis results performed on the aged samples treated with these acceleration methods described in Chapter 4, are presented and compared. Figure 5-15 and 5-16 present the results from XRF and XRD analysis, respectively. As can be seen, the electrochemical acceleration method shows an ageing effect comparable with the pH stat test and the flash column test although the specimen size is considerably larger. Application of 6 M concentrated ammonium nitrate resulted in very low Ca/Si, which may indicate a decomposition of C-S-H gel.
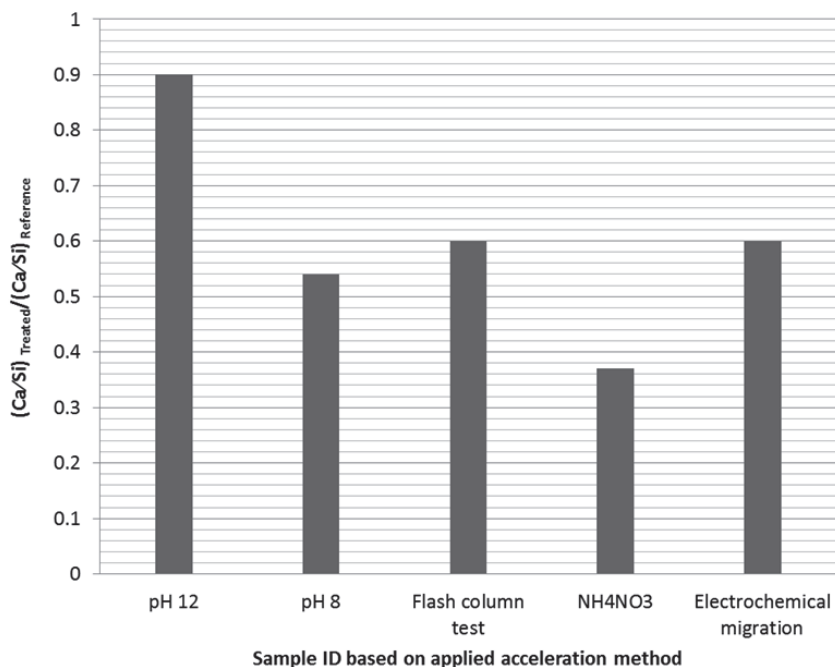


*Figure 5-15. XRF results comparing the effect of different acceleration methods on cementitious specimens*
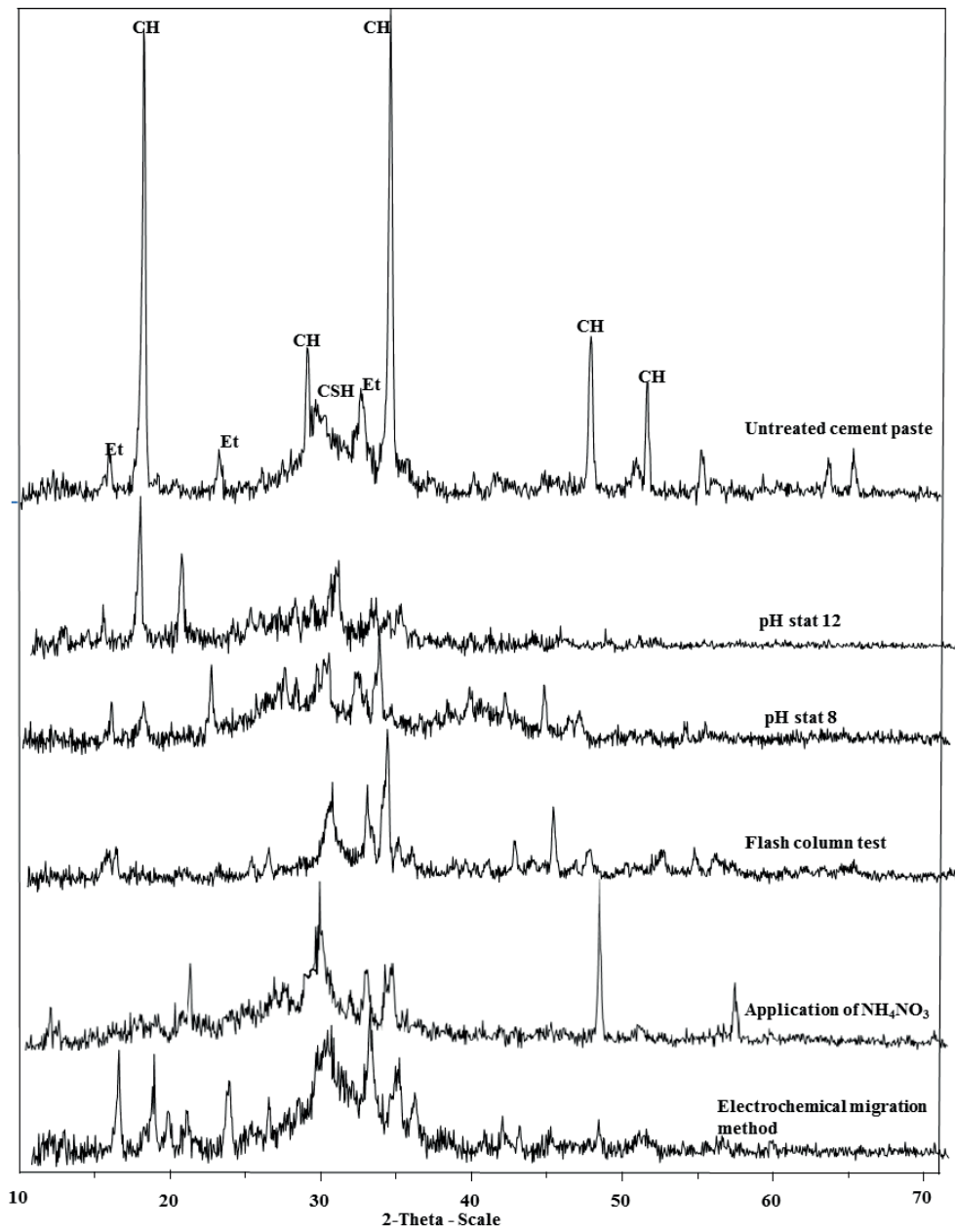
*Figure* **5-16***. XRD results comparing the effect of different acceleration methods on cementitious specimens*

# 6    Concluding remarks

The development process of an electrochemical migration method for accelerating the leaching of calcium from cementitious materials was presented. The aged specimen's size is sufficient enough for further evaluation of mechanical or transport properties.

One of the direct applications of this method is to be able to validate the service life predictions of the concrete structures in nuclear waste repositories. Based on the results from various trials the following conclusions can be drawn:

- Ammonium nitrate with an initial concentration of 0.3 M in a large volume (12-15 liters) is suitable as catholyte to receive the leached calcium ions and also to send nitrate ions into the specimen to favor dissolution of Portlandite.

- The catholyte solution must be recharged with additional ammonium nitrate and nitric acid to neutralize the cathode-released $OH^-$ and maintain the pH value in the rage of 7-9 in the catholyte.

- Lithium hydroxide with an initial concentration of 2 M in a relatively small volume (about 200 ml) is suitable as anolyte for compensating the cations and neutralizing the anode-released $H^+$ under certain test duration.

- The anolyte solution must be recharged with additional lithium hydroxide during the entire test period to maintain the pH > 14 in the anolyte.

- In order to homogenize the effect of electrical gradient on leaching the specimen should be turned upside down halfway of the experimental time.

- An imposed current with a test duration corresponding to approximately 3700 Coulombs per gram of cement paste leads to 90 percent leaching of the Portlandite content without significant destructions of the other hydrates such as C-S-H gel and Ettringite in the specimens.

- The leached specimen has a layered structure in the cross section of the specimen with a grayish layer in the middle with high Ca/Si, showing the propagation of dissolution front in time, a blackish circle with lower Ca/Si and enriched Ettringite compared with the other layers and a brownish outer layer with the lowest Ca/Si and low content of aluminum and iron.

- The topography of the aged specimen shows an increasing trend in porosity towards the curved surface of the specimen, which means higher porosity with in higher degree of leaching.

- The leaching rate with the application of the developed electro-chemical migration method can be accelerated by more than 600 times as compared with the natural leaching.

# 7 Future work

A direct application of the presented acceleration method is to study the mechanical and physical properties of the aged specimens. Moreover thermodynamic modeling should be used to predict the ageing function of the method in order to validate the service life predictions of the concrete structures in nuclear waste repositories. The planed future work in this project:

- Diffusion properties of young and aged cementitious specimens (a preliminary study regarding the diffusion properties of the young cementitious specimens is presented in Paper ii, mentioned in the publication list).
- Mechanical properties of young and aged cementitious specimens
- The freezing properties of young and aged specimens
- Permeability of young and aged specimens
- Thermodynamically modeling for study of the ageing function of the accelerated ageing method.

# 8    References

[1]     A. Gordon, *Safety analysis SFR 1, Long-term safety* SKB Rapport R-08-130, December 2008

[2]     M. Emborg, J.-E. Johansson and S. Knutsson, *Långtidsstabilitet till följd av frysning och tining av betong och bentonit vid förvaring av låg-och medelaktivt kärnavfall i SFR 1*, SKB Report R-07-60, Svensk Kärnbränslehantering AB, 2007

[3]     L.-O. Höglund, *Project SAFE: Modeling of long-term concrete degradation processes in the Swedish SFR repository*, SKB Report R-01-08, Svensk Kärnbränslehantering AB, 2001

[4]     P. Domone and J. Illistone, *Construction Materials, Their Nature and Behaviour*. 4th. ed2010.

[5]     R.H. Bogue, *Chemistry of Portland Cement* 1995, Van Nostrand Reinhold, New York.

[6]     P. Brown and J. Bothe Jr, *The system CaO-Al2O3-CaCl2-H2O at 23±2 °C and the mechanisms of chloride binding in concrete,* Cement and Concrete Research. 34 (2004) 1549-1553.

[7]     P.W. Brown and S. Badger, *The distributions of bound sulfates and chlorides in concrete subjected to mixed NaCl, MgSO4, Na2SO4 attack,* Cement and Concrete Research. 30 (2000) 1535-1542.

[8]     F. Barberon, V. Baroghel-Bouny, H. Zanni, B. Bresson, J.-B. D'espinose De La Caillerie, L. Malosse and Z. Gan, *Interactions between chloride and cement-paste materials,* Magnetic Resonance Imaging. 23 (2005) 267-272.

[9]     E.P. Nielsen, D. Herfort and M.R. Geiker, *Binding of chloride and alkalis in Portland cement systems,* Cement and Concrete Research. 35 (2005) 117-123.

[10]    O. L, Höglund, A.Bengston, *Progress Report SFR 91-06, Some Chemical and Physical Progress Related to The Long-Term Performance of The SFR repository*, KEMAKTA Consultants Co. Stockholm October 1991

[11]    C. Gervais, A.C. Garrabrants, F. Sanchez, R. Barna, P. Moszkowicz and D.S. Kosson, *The effects of carbonation and drying during intermittent leaching on the release of inorganic constituents from a cement-based matrix,* Cement and Concrete Research. 34 (2004) 119-131.

[12]    M.D. Cohen, *Theories of expansion in sulfoaluminate - type expansive cements: Schools of thought,* Cement and Concrete Research. 13 (1983) 809-818.

[13]    P.K. Mehta, *Mechanism of sulfate attack on portland cement concrete - Another look,* Cement and Concrete Research. 13 (1983) 401-406.

[14]    I. Odler and M. Gasser, *Mechanism of sulfate expansion in hydrated Portland cement,* Journal of the American Ceramic Society. 71 (1988) 1015-1020.

[15]    E.J. Reardon, *Problems and approaches to the prediction of the chemical composition in cement/water systems,* Waste Management. 12 (1992) 221-239.

[16]    U.R. Berner, *Evolution of pore water chemistry during degradation of cement in a radioactive waste repository environment,* Waste Management. 12 (1992) 201-219.

[17]    M. Hinsenveld, *A Shrinkage Core Model as a Fundamental Representation of Leaching Mechanism in Cement Stablized Waste, Doctoral Thesis*, 1992: Department of Civil and Environmental Engineering, University of Cincinnati, Cincinnati, OH.

[18]  K. Yokozeki, K. Watanabe, N. Sakata and N. Otsuki, *Modeling of leaching from cementitious materials used in underground environment,* Applied Clay Science. 26 (2004) 293-308.

[19]  F. Adenot and M. Buil, *Modelling of the corrosion of the cement paste by deionized water,* Cement and Concrete Research. 22 (1992) 489-496.

[20]  C. Carde and R. François, *Effect of the leaching of calcium hydroxide from cement paste on mechanical and physical properties,* Cement and Concrete Research. 27 (1997) 539-550.

[21]  F.H. Heukamp, F.J. Ulm and J.T. Germaine, *Mechanical properties of calcium-leached cement pastes: Triaxial stress states and the influence of the pore pressures,* Cement and Concrete Research. 31 (2001) 767-774.

[22]  H. Saito and A. Deguchi, *Leaching tests on different mortars using accelerated electrochemical method,* Cement and Concrete Research. 30 (2000) 1815-1825.

[23]  J.-S. Ryu, N. Otsuki and H. Minagawa, *Long-term forecast of Ca leaching from mortar and associated degeneration,* Cement and Concrete Research. 32 (2002) 1539-1544.

[24]  H. Saito, S. Nakane, S. Ikari and A. Fujiwara, *Preliminary experimental study on the deterioration of cementitious materials by an acceleration method,* Nuclear Engineering and Design. 138 (1992) 151-155.

[25]  F.H. Wittmann, *Corrosion of Cement-Based Materials under the Influence of an Electric Field,* Materials Science Forum. 247 (1997) 107-126.

[26]  F.-J. Ulm, E. Lemarchand and F.H. Heukamp, *Elements of chemomechanics of calcium leaching of cement-based materials at different scales,* Engineering Fracture Mechanics. 70 (2003) 871-889.

[27]  E. Revertegat, C. Richet and P. Gégout, *Effect of pH on the durability of cement pastes,* Cement and Concrete Research. 22 (1992) 259-272.

[28]  L. Tang, *Electrically accelerated methods for determining chloride diffusivity in concrete - Current development,* Magazine of Concrete Research. 48 (1996) 173-179.

[29]  *NT BUILD 492, Concrete, Mortar and Cement-based Repair Materials: Chloride Migration Coefficient from Non-steady-state Migration Experiments*, 1999: Nordtest, Esbo, Finland

[30]  P. Cronstrand, A. Babaahmadi, L. Tang and Z. Abbas. *Electrochemical leaching of cementitious materials: an experimental and theoretical study. 1st International Symposium on Cement-Based Materials for Nuclear Wastes, NUMCEM* 2011. Session 3 (Paper O344) pp. 15

[31]  H.S.a.S. Nakane, *Comparison between Diffusion Test and Electromechanical Acceleration Test for Leaching Degradation of Cement Hydration Products,* Materials Journal. 96 (1999) 208-212.

[32]  Z. Abbas, E. Ahlberg and S. Nordholm, *Monte Carlo Simulations of Salt Solutions: Exploring the Validity of Primitive Models,* The Journal of Physical Chemistry B. 113 (2009) 5905-5916.

[33]  G. Gustafson, Hagström, M. And Abbas, Z, *Beständighet av cementinjektering*, 2008: FOU.Väst Underhall av berganläggningar, Avd.f.geology och geoteknik, Chalmers teckniska högskola.

[34]  W. Pfingsten and M. Shiotsuki. *Modeling a Cement Degradation Experiment by a Hydraulic Transport and Chemical Equilibrium Coupled Code. Mat. Res. Soc. Symp.* 12/1996. 506

[35]   J. Boman, *Detector performance measurement techniques and computer software in an EDXRF-spectrometer applied to environmental and medical studies*, 1990, Göteborg University: Göteborg.